Tumour necrosis factor-α-mediated human polymeric immunoglobulin receptor expression is regulated by both mitogen-activated protein kinase and phosphatidylinositol-3-kinase in HT-29 cell line

N. Takenouchi-Ohkubo,[1] I. Moro,[2] S. Mukae,[1] Y. Kaneko[1] and K. Komiyama[1]

[1]*Department of Pathology, Nihon University, School of Dentistry, Tokyo, Japan and* [2]*Advanced Research Institute for the Sciences and Humanities, Nihon University, Tokyo, Japan*

doi:10.1111/j.1365-2567.2007.02716.x
Received 5 March 2007; revised 25 July 2007; accepted 14 August 2007.
Correspondence: Dr N. Takenouchi-Ohkubo, Department of Pathology, Nihon University, School of Dentistry, 1-8-13, Kanda-Surugadai, Chiyoda-ku, Tokyo 101–8310, Japan. Email: takenouchi@dent.nihon-u.ac.jp
Senior author: Nobuko Takenouchi-Ohkubo

Summary

Human polymeric immunoglobulin receptor (pIgR) is present on the surface of glandular epithelium, and it plays a crucial role in the mucosal immune defence. pIgR expression in HT-29 cells is up-regulated by one of the proinflammatory cytokines, tumour necrosis factor (TNF)-α. However, the mechanism used by the TNF-α-mediated signalling pathway has not been examined exclusively. To elucidate this mechanism in detail, HT-29 cells were cotreated with TNF-α and mitogen-activated protein kinase kinase (MAPKK, also called MEK1) inhibitor, PD98059, and the amount of free secretory component (SC) secreted into the culture medium was measured. The amount of free SC stimulated by TNF-α was increased by addition of PD98059. This up-regulation occurred at the transcriptional level. The amount of SC was also up-regulated by addition of TNF-α with U0126, an inhibitor of MEK1 and MEK2. Nuclear factor (NF)-κB activity and NF-κB binding to the κB2 site localized upstream of the pIgR gene did not change after coincubation of HT-29 cells with TNF-α and PD98059. The expression level of pIgR by TNF-α was decreased by LY294002, an inhibitor of phosphatidylinositol-3-kinase (PI3K), at the transcriptional level. Extracellular signal-regulated kinase (ERK)1/2 phosphorylation and NF-κB binding to the κB2 site were not affected by LY294002 treatment. These data suggest that TNF-α-mediated pIgR expression is negatively regulated by ERK pathway, which is independent of NF-κB. In addition, decrease of SC production by Ly294002 suggests that the presence of PI3K mediated regulation of SC production.

Keywords: pIgR; TNF-α; MAPK; PI3K; NF-κB

Introduction

Tumour necrosis factor-α (TNF-α) has pleiotropic functions that include roles in cell growth, differentiation, inflammatory effects, tumorigenesis, and viral replication.[1] TNF-α has been identified as the most important cytokine in the pathogenesis of inflammatory bowel disease (IBD).[2] The effect of TNF-α is mediated through two types of receptors, TNF-receptor (TNFR) 1 (also known as p55TNFR) and TNFR2 (also known as p75TNFR). TNF-α binding to these receptors activates transcription factors such as nuclear factor (NF)-κB or AP-1 that control multiple gene expressions of inflammatory cytokines such as interleukin (IL)-1, IL-6, and IL-8. TNF-α signals mediated through the TNFRs are followed by activation of mitogen-activated protein kinase (MAPK) pathways, including extracellular signal-regulated kinases (ERKs), p38, and c-Jun NH_2-terminal kinases.[3]

Human polymeric immunoglobulin receptor (pIgR) is a 120 000 MW glycoprotein present on glandular epithelial

Abbreviations: ELISA, enzyme-linked immunosorbent assay; EMSA, electrophoretic mobility shift assay; ERK, extracellular signal-regulated kinase; IBD, inflammatory bowel disease; IL-1β, interleukin-1 β; IL-6, interleukin-6; IL-8, interleukin-8; IFN-γ, interferon-γ; IRF-1, IFN-γ regulatory factor-1; MAPK, mitogen-activated protein kinase; MEK, MAPK/ERK kinase; NF-κB, nuclear factor-κB; PI3K, phosphatidylinositol-3-kinase; pIgR, polymeric immunoglobulin receptor; SC, secretory component; S-IgA, secretory immunoglobulin A; TNF-α, tumor necrosis factor-α; TNFR, TNF-receptor.

cells that functions as a receptor for polymeric immunoglobulin (pIg). pIgR transports polymeric immunoglobulin A (IgA) into external secretions as secretory IgA (S-IgA), which is critical for the defence of mucosal tissues.[4] Free secretory component (SC) is important for the enhancement of immune responses. For example, degranulation of eosinophils caused by binding of S-IgA or SC is mediated through the 15 000 MW SC receptor expressed in eosinophils.[5,6] Degranulation of IL-3-primed basophils is also mediated by SC.[7] Free SC can bind to several bacterial proteins, such as colonization factor antigen,[8] *Clostridium difficile* toxin A,[9] and *Streptococcus pneumoniae* protein SpsA.[10–12] Interferon-γ (IFN-γ),[13] TNF-α,[14] IL-4[15] and IL-1β[16] can up-regulate the release of SC into the culture supernatant of the human colonic adenocarcinoma cell line, HT-29. Production of SC by IFN-γ, TNF-α, or IL-1β is regulated by IFN-γ regulatory factor-1 (IRF-1) binding to an element in exon 1 of the pIgR gene that is induced by Janus kinase/signal transducer and activator of transcription (STAT) cascade or NF-κB.[17–19] In addition, IL-4 and IFN-γ synergistically increased the release of SC in HT-29 cells.[15] These data indicate that pIgR expression is regulated by cytokines.

We hypothesized that the activation of ERK contributes to the TNF-α–induced pIgR gene expression. Treatment of HT-29 cells with TNF-α up-regulates the SC production at the transcriptional level, as previously described.[14,20] However, cotreatment of HT-29 cells with TNF-α and MAPK kinase (MAPKK, also called MEK1) inhibitor, PD98059, enhanced the TNF-α–induced SC production. Our data suggest that the production of SC in HT-29 cells is also regulated by a negative effect that is involved in ERK activation.

Materials and methods

cDNA

Human pIgR[21–23] cDNA was kindly provided by Prof. P. Brandtzeag (LIIPAT, Institute of Pathology, National Hospital, University of Oslo, Oslo, Norway). As a probe for Northern blot analysis, *Pst*I (668-bp) fragments were used for the detection of pIgR mRNA.

Reagents

Recombinant human TNF-α (specific activity = 2×10^7 U/mg) was purchased from Genzyme Corp. (Cambridge, MA). 2′-amino-3′-1,4-diamino-2,3-dicyano-1 methoxyflavone (PD98059),[24] 4-bis[2-aminophenylthio]butadiene (U0126),[25] 2-(4-morpholinyl)-8-phenyl-4H-1-benzopyran-4-one (LY294002)[26] and antibodies against phosphoERK1/2 (anti-ACTIVE MAPK) and ERK1/2 were purchased from Promega Corp. (Madison, WI).

Cell culture

A human colonic adenocarcinoma cell line, HT-29, was maintained in MaCoy's 5 A medium (Life Technologies Inc., Gaithersburg, MD) supplemented with 10% fetal calf serum (Cansera International Inc., Ontario, Canada), 1 mM glutamine (Life Technologies Inc., Gaithersburg, MD), amphotericin B, and penicillin/streptomycin (Life Technologies Inc., Gaithersburg, MD) at 37° in an atmosphere of humidified 5% CO_2. We selected HT-29 cell line because this cell line has been often used to examined the mechanisms of SC production by TNF-α[20,30,31,32] and we considered that HT-29 is a very good pIgR expression model. In addition and there is no appropriate cell line to use this study. Prior to treatment, cells (1×10^6 cells/ml) were plated with fresh medium and cultured. On the second day after plating, 10 ng/ml of human recombinant TNF-α, with or without PD98059, U0126, or LY294002, was added to the medium of the serum-free condition, and cultivation continued for 48 hr. Then, cultured cells were harvested, and 2 ml of Solution D was added for RNA extraction.[27] The supernatants were also collected and subjected to enzyme-linked immunosorbent assay (ELISA), as previously described.[16,28] All experiments were performed in triplicate, and differences between means were calculated using Student's *t*-test.

Northern blot analysis

Ten μg of total RNA was mixed with loading buffer {50% formamide, 6% formalin, 1 × Goldberg buffer [40 mM Na-MOPS pH 7·2, 5 mM sodium acetate, 0·5 mM ethylenediamine N,N,N′,N′tetra-acetic acid (EDTA)]}, denatured at 65° for 15 min, and cooled on ice. Then, RNA was electrophoresed through a 1·0% agarose gel containing 6% formalin. After electrophoresis, the gel was neutralized by incubation with 0·25 M ammonium acetate solution for 5 min, and the RNA was transferred onto Hybond-N (Amersham, Little Chalfont, UK). The RNA was fixed to the membrane by using a UV crosslinker. Before hybridization, the membrane was incubated in prehybridization solution [50% formamide, 0·65 M NaCl, 5 mM EDTA (pH 7·5), 0·1% sodium dodecyl sulphate (SDS), 0·1 M piperazine-N,N′-bis-[2-ethanesulfonic acid] (PIPES) [pH 6·8], 5× Denhardt's solution] at 42° for 6 hr. The hybridization probe was prepared by using a random prime DNA labelling kit (TAKARA Shuzo Co., Shiga, Japan) and purified by Sephadex G-50 (Pharmacia Biotech, Uppsala, Sweden). For hybridization, dextran sulfate (Pharmacia Biotech) was added to the prehybridization solution at a final concentration of 10%. After hybridization, the membrane was washed four times with washing buffer (2× standard sodium citrate, 0·1% SDS, 0·2% sodium pyrophosphate) at 55° for 30 min and exposed to X-OMAT film (Kodak, Rochester, NY) at −80°.

Reverse trranscription–polymerase chain reaction (RT–PCR)

Cells treated with LY294002 and/or TNF-α were collected and total RNA was extracted by RNeasy (Qiagen, Valencia, CA). After extraction of total RNA, 500 ng of total RNA was used for cDNA synthesis using SuperScript III reverse transcriptase (Invitrogen, San Diego, CA) as manufacture's instruction. Then, 2 μl of synthesized cDNA was used as a template for RT–PCR. The sequence of primer is as following; human pIgR hSC3 5′-TTGTCT CCCTGACCCTGAAC-3′, hSC4; 5′-CAAATTCCCTGG AGTTCTCG-3′ (product size is 501 bp), β-actin BACT F 4TH; 5′-TTCCAGCCTTCCTTCCTGG-3′, β-actin BACT R 4TH; 5′-TTGCGCTCAGGAGGAGCAA-3′ (product size is 225 bp).Amplification of human SC and β-action was performed using HotMasterMix (Eppendorf) as following condition; 94° for 3 min, then, 94° for 30 s, 60° for 30 s, 72° for 30 s for 35 cycles. Then PCR product was incubated for 8 min at 72° and stored at 4°.

Electrophoretic mobility shift assay (EMSA)

Nuclear extracts were prepared by the method as described previously.[20] For preparation of the probe, synthetic oligomers ([κB2, corresponding to −461∼–440; 5′-GATCGTCGGAGGGGATTCCAGAGCAA-3′, 3′-CAG CCTCCCCTAAGGTCTCGTTCTAG-5′) were annealed and radiolabelled with the Klenow fragment of DNA polymerase I and [α-^{32}P] dCTP (Amersham). For the binding reaction, 10 μg of nuclear extract was incubated in 22 μl of a buffer containing 25 mM HEPES (pH 7·9), 2 mM EDTA (pH 8·0), 50 mM KCl, 10% glycerol, 2 μg of poly dI-dC (Pharmacia Biotech), 1% bovine serum albumin (BSA), and 10^4 counts per minute (c.p.m.) of radiolabelled probe for 30 min at 30°. After the reaction, 1 μl of loading buffer (5% glycerol, 50 mM EDTA [pH 8·0], 0·05% bromophenol blue, 0·05% xylene cyanol) was added and separated through a 6% native polyacrylamide gel in TAE buffer (67 mM Tris, 33 mM sodium acetate [pH 6·0], 10 mM EDTA) at room temperature. The gel was then dried and exposed to Kodak X-OMAT film at −80° for 12 hr.

Preparation of cell lysate and SDS–Polyacrylamide gele electrophoresis (PAGE)

For analysis of phosphorylated ERK, HT-29 cells were treated with TNF-α with or without PD98059 at 37° for 15 min and 48 hr. Then, cells were washed with PBS and lysed in cell lysis buffer (20 mM Tris, pH 7·5, 150 mM NaCl, 0·25 M sucrose, 5 mM EDTA, 5 mM ethylene glycole bis-(β-aminoethyl ether)-N,N,N′-N′-tetraacetic acid (EGTA), 0·5% Triton-X-100, 25 mM NaF, 5 mM Na_3VO_4, 5 mM β-glycerophosphate, 1·5 mM phenylmethylsulphonyl fluoride, 5 μg/ml leupeptin, 10 μg/ml aprotinin),[29] and the soluble fraction was collected by centrifugation at 20 000 ***g*** at 4° for 15 min. Protein concentration was measured by a Bio-Rad Protein assay kit (Bio-Rad Laboratories, Hercules, CA). Fifty μg of protein was separated by 10% SDS–PAGE.

Western blot analysis

After electrophoresis, the gel was incubated with transfer buffer (24·8 mM Tris, 192·5 mM glycine, 0·05% methanol) for 30 min and transferred onto Immobilon P (Millipore, Bedford, MA) by electroblot. The membrane was incubated in blocking buffer (1% BSA in TBST [20 mM Tris-HCl pH 7·5, 150 mM NaCl, 0·05% Tween 20]) at room temperature for 12 hr. Detection of MAPKs was performed using anti-active MAPK antibody as a primary antibody, donkey anti-rabbit IgG conjugated with alkaline phosphatase as a secondary antibody, and CDP-Star reagent for signal detection (Amersham). For reprobing, the membrane was incubated with stripping buffer (100 mM 2-mercaptoethanol, 2% SDS, 62·5 mM Tris-HCl, pH 6·8) at 50° for 30 min and washed twice with TBST at room temperature for 10 min. Then, the membrane was incubated with blocking buffer at room temperature for 16 h and subjected to immunodetection using anti-ERK1/2 antibody.

Results

Production of SC by TNF-α is enhanced by PD98059

To elucidate whether the MAPK is involved in TNF-α signalling and SC production, HT-29 cells were incubated with TNF-α for 48 h with 0, 5, 25, or 50 μM of PD98059. Then, ELISA was performed on culture supernatants to quantify the amount of SC. The amount of SC is enhanced by TNF-α as compared to the control, as described previously (data not shown). This effect was enhanced significantly by addition of PD98059 ($P < 0·002$ when concentration is 50 μM) (Fig. 1a). The same effect was also observed by pretreatment of HT-29 with PD98059 for 30 min followed by stimulation of TNF-α for 48 hr (data not shown). SC production by TNF-α was also significantly up-regulated by cotreatment with U0126, an inhibitor of MEK1/2 ($P < 0·01$ when concentration is 1 μM) (Fig. 1b).

Enhancement of SC production by PD98059 is regulated at the transcriptional level

To determine if the enhancement of SC production by PD98059 is regulated at the transcriptional level or translational level, HT-29 cells were treated with TNF-α and 5 μM of PD98059 for 48 hr, and northern blot analysis was performed. The expression of pIgR mRNA induced by TNF-α was increased by PD98059 (Fig. 2).

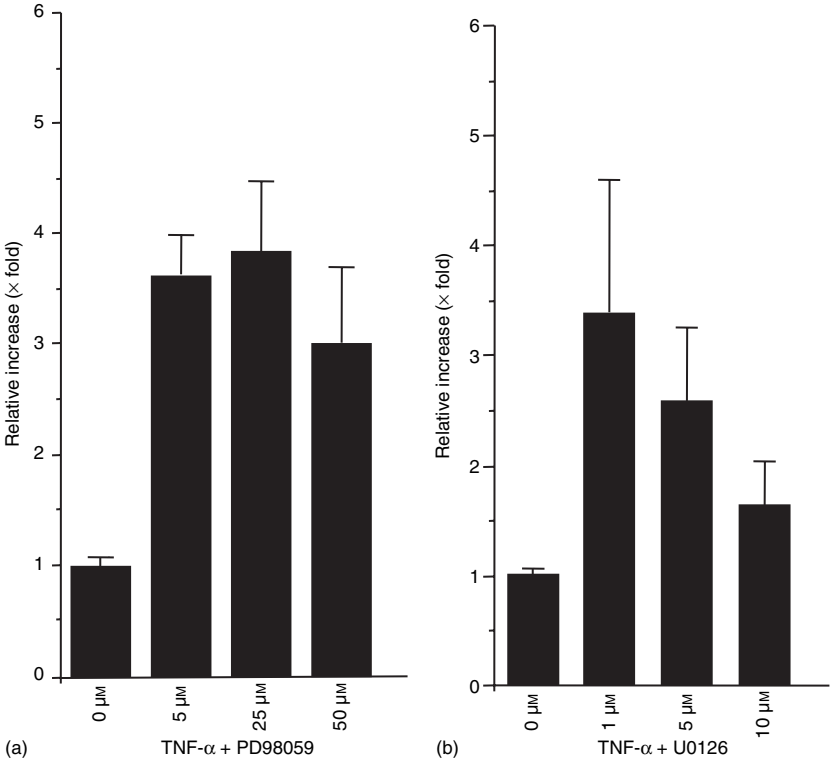

Figure 1. Production of SC by TNF-α is up-regulated by addition of MEK1 inhibitor, PD98059 (a) or MEK1/2 inhibitor U0126 (b) in a concentration-dependent manner. HT-29 cells were treated with 10 ng/ml of TNF-α and 0, 5, 25, or 50 μM of PD98059 (a) or 0, 1, 5, or 10 μM of U0126 (b) and cultured for 48 hr. Then, supernatants were subjected to ELISA, and the amounts of SC were measured.

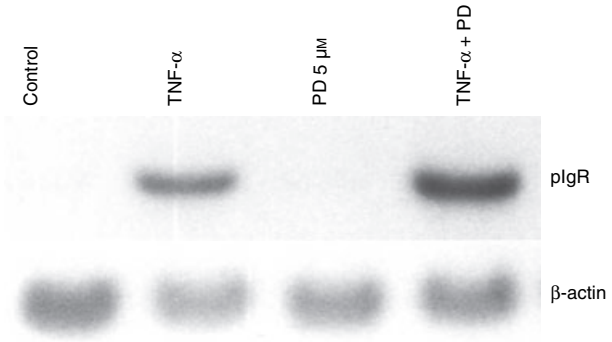

Figure 2. Enhancement of SC by TNF-α and PD98029 is controlled at the transcriptional level. HT-29 cells were treated with TNF-α and 5 μM of PD98059 or 1 μM of U0126 or DMSO for 48 hr. Then, total RNA was extracted and 10 μg of total RNA was subjected to northern blot analysis using human pIgR cDNA.

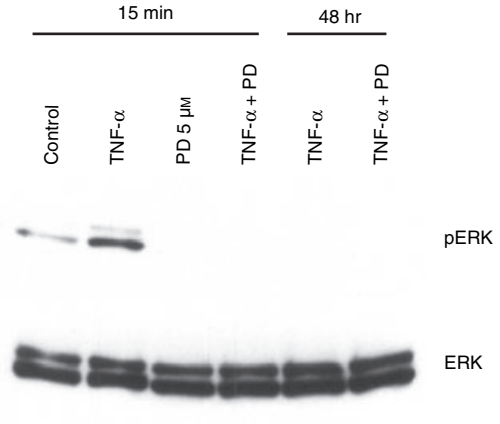

Figure 3. Phosphorylation of ERK1/2 by TNF-α is blocked by 5 μM of PD98059. HT-29 cells were treated with 10 ng/ml of TNF-α and 5 μM of PD98059 or DMSO for 15 min. Then, protein was extracted and phosphorylated ERK1/2 was detected by Western blot using antiactive ERK antibody. To check the amount of total ERK1/2, anti-ERK1/2 antibody was used.

ERK is activated by TNF-α in HT-29 and inhibited by PD98059, a MEK inhibitor

To check whether TNF-α-activated ERK1/2 was inhibited by PD98059, HT-29 cells were treated with TNF-α for 15 min and 48 hr with or without PD98059. Cell lysates were collected, and phosphorylated ERK1/2 was detected by western blotting analysis. When HT-29 cells were treated with TNF-α for 15 min, both ERK1 and ERK2 were phosphorylated as previously reported[33] and after 48 hr, the amount of phosphorylated ERK1/2 was decreased. Activation of ERK1/2 by TNF-α was completely inhibited by treatment with 5 μM of PD98059 (Fig. 3). The amount of ERK protein did not change by treatment of TNF-α with or without PD98059 (Fig. 3).

SC production by TNF-α is inhibited by phosphatidylinositol-3-kinase (PI3K) inhibitor LY294002

PI3K is also activated by extracellular signals such as growth factors, cytokines, integrin-mediated signals, and

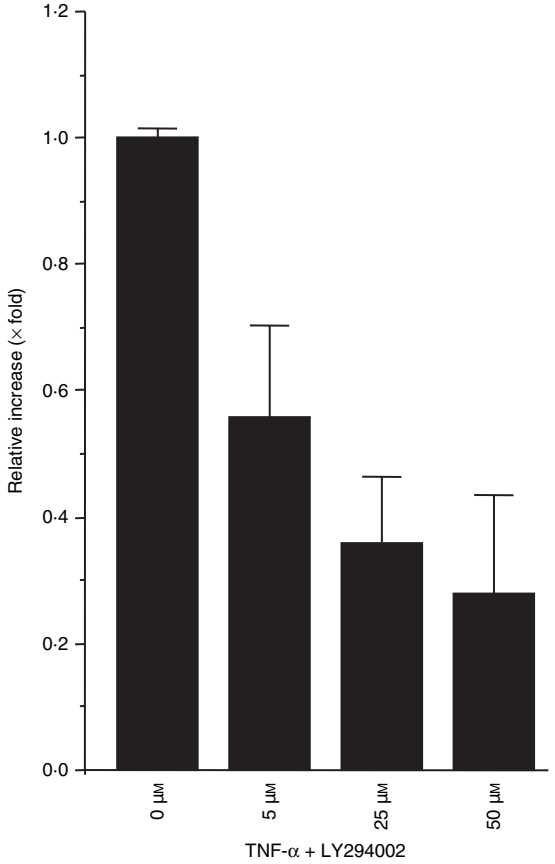

Figure 4. SC production by TNF-α is inhibited by LY294002.HT-29 cells were treated with 10 ng/ml of TNF-α with 0, 5, 25, or 50 μM of LY294002 for 48 hr. Then, supernatants were subjected to ELISA, and the amounts of SC were measured.

other survival signals.[34] To elucidate whether PI3K is involved in TNF-α–induced SC production, HT-29 cells were costimulated with TNF-α and LY294002 for 48 hr, and then the amount of SC protein in culture supernatants was quantified. The production of SC was inhibited by PI3K inhibitor as previously reported[35,36] at any concentration, especially at the 50 μM concentration (Fig. 4).

Inhibition of SC production by LY294002 is regulated at the transcriptional level

It has been indicated that PI3K inhibitor inhibit transcytosis of pIgR.[35,36] To check whether inhibition of pIgR by LY294002 is regulated at the transcriptional or post-transcriptional level, RT–PCR was performed. As we showed the decrease of SC production by LY294002, expression level of pIgR mRNA was also decreased as compared with TNF-α stimulation. This data suggest that inhibition of SC production by LY294002 was regulated at the transcriptional level (Fig. 5). Treatment of HT-29 with only LY294002 completely inhibited the expression of SC mRNA as compared with control, which express

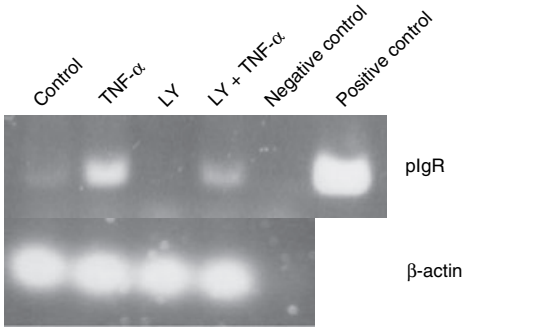

Figure 5. TNF-α mediated SC production inhibited by LY294002 is regulated at the transcriptional level. HT-29 cells were treated with LY294002 and TNF-α for 48 hr. Then total RNA was extracted and RT–PCR was performed to detect pIgR mRNA. For positive control of pIgR, 2 ng of full length pIgR cDNA was used.

free SC constitutively, suggesting that LY294002 inhibited mainly constitutively expressed pIgR mRNA.

Involvement of NF-κB in the enhancement of SC production by PD98059 and inhibition by Ly294002

Treatment of glioblastoma cell line T98G with PD98059 and IL-1β augmented NF-κB activation.[37] NF-κB is an important transcription factor for the pIgR gene.[20,30–32] We checked whether the enhanced SC production by PD98059 is via enhanced NF-κB activation by using a gel shift assay to detect the NF-κB bound upstream of the pIgR gene (κB2). The amount of NF-κB binding to the κB2 site did not increase after PD98059 treatment (Fig. 6). We also checked whether inhibition of PI3K influences the effect of NF-κB activation. HT-29 cells were treated with 10 ng/ml of TNF-α with or without LY294002 for 90 min, and then nuclear extracts were prepared and the gel shift assay was performed using κB2 probe. Co-treatment of HT-29 cells with TNF-α and LY294002 did not change the binding of NF-κB to κB2 (Fig. 6).

Inhibition of PI3K by TNF-α is independent of ERK activation

To determine if inhibition of PI3K affected ERK activation, HT-29 cells were treated with 50 μM of LY294002 for 15 min. Cell lysates were applied to western blots. The amount of phosphorylated ERK was unchanged by cotreatment with TNF-α and LY294002 (Fig. 7).

Discussion

In IBD such as Crohn's disease and ulcerative colitis, the number of TNF-α-producing cells is increased in the small intestine.[2] Some treatment strategies for IBD target TNF using anti-TNF monoclonal antibody (infliximab)[38] or MAPK signalling pathway inhibitor (CNI-1493).[39] On

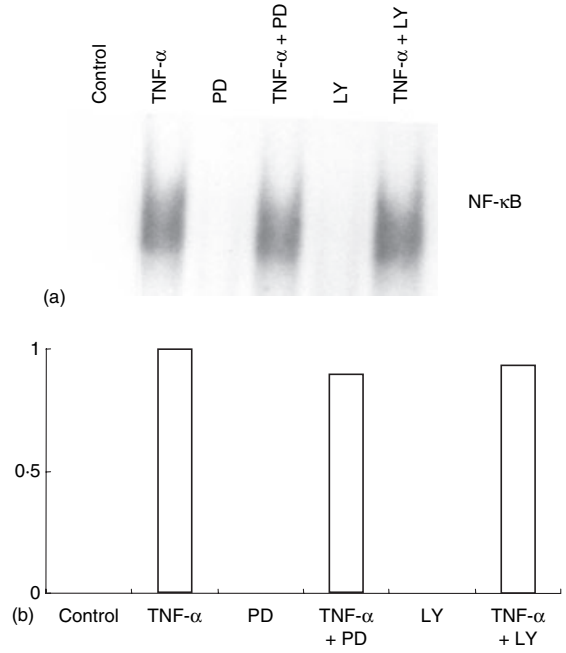

Figure 6. Binding of NF-κB to κB2 is not affected by PD98059 and LY294002. (a) HT-29 cells were treated with 10 ng/ml of TNF-α and 5 μM of PD98059 or 50 μM of LY294002 for 90 min, and then nuclear protein was extracted. Ten μg of nuclear protein was used for the gel shift assay. (b) Densitometric analysis of gel shift assay using Image J software. *Y*-axis shows the density of band compared to TNF-α stimulation (= 1) as a control.

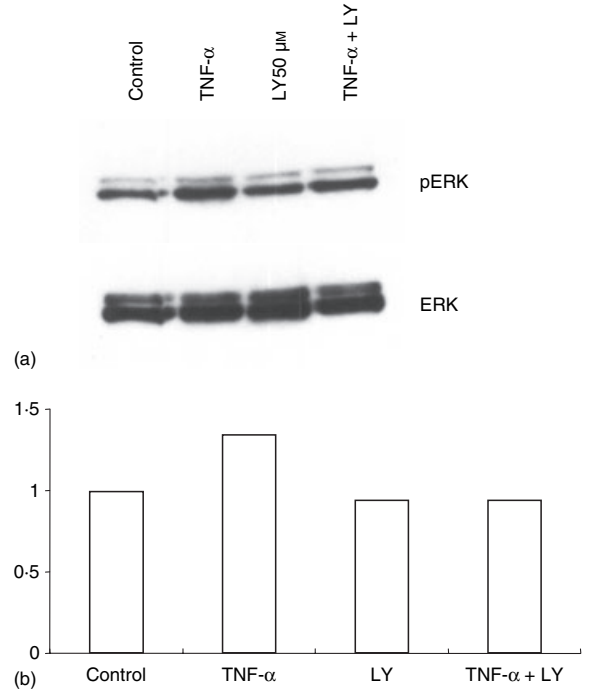

Figure 7. Activation of ERK by TNF-α was not altered by LY294002. (a) HT-29 cells were treated with 10 ng/ml of TNF-α and 50 μM of LY294002 for 15 min. Then, protein was extracted and phosphorylated ERK1/2 was detected by Western blot using antiactive ERK antibody. (b) Densitometric analysis using Image J software.

the other hand, the expression levels of pIgR and S-IgA were decreased in IBD.[40] In lung epithelial cells, expression of SC is reduced in chronic obstructive pulmonary disease[41] and in this condition SC is cleaved by serine protease produced by phorbol myristate-activated polynuclear neutrophil (PMN).[42]

In this study, we reported that production of SC by TNF-α was enhanced by MEK1/2 inhibitors (Fig. 1) without the redundant NF-κB activation (Fig. 6). Our data suggest that MAP kinase signalling pathway inhibitor is a beneficial treatment for IBD because there is a possibility that the decreased pIgR protein and S-IgA would be elevated and that might enhance the mucosal immunity without excessive NF-κB activation.

There are several reports about the signalling mechanisms that enhance the expression level of pIgR by various cytokines. When HT-29 cells are treated with IFN-γ and IL-4, the expression level of pIgR mRNA is up-regulated, and protein tyrosine kinase is involved in up-regulation of pIgR.[43] In addition, the STAT-6 binding site located at intron 1 is important for the up-regulation of pIgR gene expression by IL-4[44] and co-operation of STAT-6 and tissue-specific factor, hepatocyte NF-1, is also required.[45] PIgR gene expression induced by TNF-α has also been suggested to be regulated by NF-κB located upstream of the transcription initiation site[20] and another binding site located at intron 1[45] is strongly suggested to be involved. However, signalling mechanisms by TNF-α were not well elucidated.

ERKs were activated by treatment of HT-29 cells with TNF-α (Fig. 3), and production of SC by TNF-α was enhanced by inhibition of ERKs (Fig. 1). These data indicate the existence of a negative regulation pathway by TNF-α stimulation. In addition, PI3K inhibition by LY294002 decreased the production of SC by TNF-α (Fig. 4) without NF-κB inactivation (Fig. 6) and ERK activation (Fig. 7), suggesting that the PI3K pathway positively regulates SC production at the transcriptional level. As it has been reported that PI3K is involved in transcytosis of pIgR[35,36] inhibition of SC production by PI3K inhibitor is controlled at the transcriptional level (Fig. 5). We could not detect SC production by ELISA from the control sample but could detect by RT–PCR, probably depending on the different sensitivities of detection system. These data suggest that PI3K is involved in trancytosis of pIgR in the HT-29 cells as previously indicated[8,35,36] and our data confirm previous data. Because we have indicated that expression of pIgR mRNA was not completely inhibited by NF-κB inhibitor[20] it is possible that there is also an NF-κB-independent pathway. In bronchial epithelial cells, up-regulation of SC production by activated PMN was also inhibited by NF-κB and p38 inhibitor. However, activation of NF-κB and p38 is independent of SC production by serine proteinase, which means that SC cleavage and expression are independently

regulated.[42] Our data indicate that there are several kinds of signalling pathways, such as NF-κB-dependent and NF-κB-independent pathways, which are involved in SC production by TNF-α. Our data also indicate the existence of negative and positive regulators of the NF-κB-independent pathway in HT-29 cells. Further investigations are needed to elucidate the complicated mechanisms of signalling pathways for SC production.

Acknowledgements

Financial support was obtained from the Nihon University Research Grant for Assistants and Young Researchers (2003), the Grant from the Ministry of Education, Culture, Sports, Science and Technology to promote multidisciplinary research projects, and Academic Frontier Project for Private Universities: matching fund subsidy from MEXT (to Dr Hiroki Nagase).

References

1 Wajant H, Pfizenmaier K, Scheurich P. Tumor necrosis factor signaling. *Cell Death Differ* 2003; **10**:45–65.
2 Breese EJ, Michie CA, Nicholls SW, Murch SH, Williams CB, Domizio P, Walker-Smith JA, MacDonald TT. Tumor necrosis factor alpha-producing cells in the intestinal mucosa of children with inflammatory bowel disease. *Gastroenterology* 1994; **106**: 1455–66.
3 MacEwan DJ. TNF ligands and receptors – a matter of life and death. *Br J Pharmacol* 2002; **135**:855–75.
4 Mestecky J, McGhee JR. Immunoglobulin A (IgA). molecular and cellular interactions involved in IgA biosynthesis and immune response. *Adv Immunol* 1987; **40**:153–245. 153–245.
5 Motegi Y, Kita H. Interaction with secretory component stimulates effector functions of human eosinophils but not of neutrophils. *J Immunol* 1998; **161**:4340–6.
6 Lamkhioued B, Gounni AS, Gruart V, Pierce A, Capron A, Capron M. Human eosinophils express a receptor for secretory component. Role in secretory IgA-dependent activation. *Eur J Immunol* 1995; **25**:117–25.
7 Iikura M, Yamaguchi M, Fujisawa T *et al.* Secretory IgA induces degranulation of IL-3-primed basophils. *J Immunol* 1998; **161**: 1510–5.
8 de Oliveira IR, de Araujo AN, Bao SN, Giugliano LG. Binding of lactoferrin and free secretory component to enterotoxigenic *Escherichia coli*. *FEMS Microbiol Lett* 2001; **203**:29–33.
9 Dallas SD, Rolfe RD. Binding of *Clostridium difficile* toxin A to human milk secretory component. *J Med Microbiol* 1998; **47**:879–88.
10 Hammerschmidt S, Tillig MP, Wolff S, Vaerman JP, Chhatwal GS. Species-specific binding of human secretory component to SpsA protein of *Streptococcus pneumoniae* via a hexapeptide motif. *Mol Microbiol* 2000; **36**:726–36.
11 Hammerschmidt S, Talay SR, Brandtzaeg P, Chhatwal GS. SpsA, a novel pneumococcal surface protein with specific binding to secretory immunoglobulin A and secretory component. *Mol Microbiol* 1997; **25**:1113–24.
12 Elm C, Rohde M, Vaerman JP, Chhatwal GS, Hammerschmidt S. Characterization of the interaction of the pneumococcal surface protein SpsA with the human polymeric immunoglobulin receptor (hpIgR). *Indian J Med Res* 2004; **119** (Suppl.):61–5.
13 Sollid LM, Kvale D, Brandtzaeg P, Markussen G, Thorsby E. Interferon-gamma enhances expression of secretory component, the epithelial receptor for polymeric immunoglobulins. *J Immunol* 1987; **138**:4303–6.
14 Kvale D, Lovhaug D, Sollid LM, Brandtzaeg P. Tumor necrosis factor-alpha up-regulates expression of secretory component, the epithelial receptor for polymeric Ig. *J Immunol* 1988; **140**:3086–9.
15 Phillips JO, Everson MP, Moldoveanu Z, Lue C, Mestecky J. Synergistic effect of IL-4 and IFN-gamma on the expression of polymeric Ig receptor (secretory component) and IgA binding by human epithelial cells. *J Immunol* 1990; **145**:1740–4.
16 Hayashi M, Takenouchi N, Asano M, Kato M, Tsurumachi T, Saito T, Moro I. The polymeric immunoglobulin receptor (secretory component) in a human intestinal epithelial cell line is up-regulated by interleukin-1. *Immunology* 1997; **92**:220–5.
17 Piskurich JF, Youngman KR, Phillips KM, Hempen PM, Blanchard MH, France JA, Kaetzel CS. Transcriptional regulation of the human polymeric immunoglobulin receptor gene by interferon-gamma. *Mol Immunol* 1997; **34**:75–91.
18 Kaetzel CS, Blanch VJ, Hempen PM, Phillips KM, Piskurich JF, Youngman KR. The polymeric immunoglobulin receptor: structure and synthesis. *Biochem Soc Trans* 1997; **25**:475–80.
19 Blanch VJ, Piskurich JF, Kaetzel CS. Cutting edge: coordinate regulation of IFN regulatory factor-1 and the polymeric Ig receptor by proinflammatory cytokines. *J Immunol* 1999; **162**:1232–5.
20 Takenouchi-Ohkubo N, Takahashi T, Tsuchiya M, Mestecky J, Moldoveanu Z, Moro I. Role of nuclear factor-kappaB in the expression by tumor necrosis factor-alpha of the human polymeric immunoglobulin receptor (plgR) gene. *Immunogenetics* 2000; **51**:289–95.
21 Krajci P, Grzeschik KH, Geurts van Kessel AH, Olaisen B, Brandtzaeg P. The human transmembrane secretory component (poly-Ig receptor): molecular cloning, restriction fragment length polymorphism and chromosomal sublocalization. *Hum Genet* 1991; **87**:642–8.
22 Krajci P, Kvale D, Tasken K, Brandtzaeg P. Molecular cloning and exon-intron mapping of the gene encoding human transmembrane secretory component (the poly-Ig receptor). *Eur J Immunol* 1992; **22**:2309–15.
23 Krajci P, Solberg R, Sandberg M, Oyen O, Jahnsen T, Brandtzaeg P. Molecular cloning of the human transmembrane secretory component (poly-Ig receptor) and its mRNA expression in human tissues. *Biochem Biophys Res Commun* 1989; **158**:783–9.
24 Alessi DR, Cuenda A, Cohen P, Dudley DT, Saltiel AR. PD 098059 is a specific inhibitor of the activation of mitogen-activated protein kinase kinase *in vitro* and *in vivo*. *J Biol Chem* 1995; **270**:27489–94.
25 Favata MF, Horiuchi KY, Manos EJ *et al.* Identification of a novel inhibitor of mitogen-activated protein kinase kinase. *J Biol Chem* 1998; **273**:18623–32.
26 Vlahos CJ, Matter WF, Hui KY, Brown RF. A specific inhibitor of phosphatidylinositol 3-kinase, 2-(4-morpholinyl)-8-phenyl-4H-1-benzopyran-4-one (LY294002). *J Biol Chem* 1994; **269**:5241–8.

27 Chomczynski P, Sacchi N. Single-step method of RNA isolation by acid guanidinium thiocyanate-phenol-chloroform extraction. *Anal Biochem* 1987; **162**:156–9.
28 Kusama K, Takahashi T, Asano M, Iwase T, Saito T, Nagasaki Y, Moro I. Murine monoclonal antibody to secretory component. *Shika Kiso Igakkai Zasshi* 1989; **31**:471–3.
29 Ogier-Denis E, Pattingre S, El Benna J, Codogno P. Erk1/2-dependent phosphorylation of Galpha-interacting protein stimulates its GTPase accelerating activity and autophagy in human colon cancer cells. *J Biol Chem* 2000; **275**:39090–5.
30 Ackermann LW, Denning GM. Nuclear factor-kappaB contributes to interleukin-4- and interferon-dependent polymeric immunoglobulin receptor expression in human intestinal epithelial cells. *Immunology* 2004; **111**:75–85.
31 Schjerven H, Brandtzaeg P, Johansen FE. A novel NF-kappa B/Rel site in intron 1 cooperates with proximal promoter elements to mediate TNF-alpha-induced transcription of the human polymeric Ig receptor. *J Immunol* 2001; **167**:6412–20.
32 Schjerven H, Tran TN, Brandtzaeg P, Johansen FE. *De novo* synthesized RelB mediates TNF-induced up-regulation of the human polymeric Ig receptor. *J Immunol* 2004; **173**:1849–57.
33 Jijon HB, Panenka WJ, Madsen KL, Parsons HG. MAP kinases contribute to IL-8 secretion by intestinal epithelial cells via a posttranscriptional mechanism. *Am J Physiol Cell Physiol* 2002; **283**:C31–C41.
34 Fruman DA, Cantley LC. Phosphoinositide 3-kinase in immunological systems. *Semin Immunol* 2002; **14**:7–18.
35 Cardone M, Mostov K. Wortmannin inhibits transcytosis of dimeric IgA by the polymeric immunoglobulin receptor. *FEBS Lett* 1995; **376**:74–6.
36 Verges M, Sebastian I, Mostov KE. Phosphoinositide 3-kinase regulates the role of retromer in transcytosis of the polymeric immunoglobulin receptor. *Exp Cell Res* 2007; **313**:707–18.
37 Funakoshi M, Tago K, Sonoda Y, Tominaga S, Kasahara T. A MEK inhibitor, PD98059 enhances IL-1-induced NF-kappaB activation by the enhanced and sustained degradation of Ikappa-Balpha. *Biochem Biophys Res Commun* 2001; **283**:248–54.
38 Stein RB, Hanauer SB. Medical therapy for inflammatory bowel disease. *Gastroenterol Clin North Am* 1999; **28**:297–321.
39 Sandborn WJ. Strategies for targeting tumour necrosis factor in IBD. *Best Pract Res Clin Gastroenterol* 2003; **17**:105–17.
40 Marteau P, Colombel JF, Nemeth J, Vaerman JP, Dive JC, Rambaud JC. Immunological study of histologically non-involved jejunum during Crohn's disease: evidence for reduced *in vivo* secretion of secretory IgA. *Clin Exp Immunol* 1990; **80**:196–201.
41 Pilette C, Godding V, Kiss R *et al.* Reduced epithelial expression of secretory component in small airways correlates with airflow obstruction in chronic obstructive pulmonary disease. *Am J Respir Crit Care Med* 2001; **163**:185–94.
42 Pilette C, Ouadrhiri Y, Dimanche F, Vaerman JP, Sibille Y. Secretory component is cleaved by neutrophil serine proteinases but its epithelial production is increased by neutrophils through NF-kappa B- and p38 mitogen-activated protein kinase-dependent mechanisms. *Am J Respir Cell Mol Biol* 2003; **28**:485–98.
43 Denning GM. IL-4 and IFN-gamma synergistically increase total polymeric IgA receptor levels in human intestinal epithelial cells. Role of protein tyrosine kinases. *J Immunol* 1996; **156**:4807–14.
44 Schjerven H, Brandtzaeg P, Johansen FE. Mechanism of IL-4-mediated up-regulation of the polymeric Ig receptor: role of STAT6 in cell type-specific delayed transcriptional response. *J Immunol* 2000; **165**:3898–906.
45 Schjerven H, Brandtzaeg P, Johansen FE. Hepatocyte NF-1 and STAT6 cooperate with additional DNA-binding factors to activate transcription of the human polymeric Ig receptor gene in response to IL-4. *J Immunol* 2003; **170**:6048–56.

Phosphorylation of ERK in Trigeminal Spinal Nucleus Neurons Following Passive Jaw Movement in Rats with Chronic Temporomandibular Joint Inflammation

Ikuko Suzuki
Graduate Student
College of Pharmacy, Nihon University
Chiba, Japan

Toshiyuki Harada, DDS, PhD
Research Assistant
Department of Prosthodontics

Masatake Asano, DDS, PhD
Assistant Professor
Department of Pathology

Yoshiyuki Tsuboi, DDS, PhD
Assistant Professor
Department of Physiology

Masahiro Kondo, DDS, PhD
Assistant Professor
Department of Physiology

Nobuhito Gionhaku, DDS, PhD
Professor
Department of Prosthodontics

Nihon University School of Dentistry
Tokyo, Japan

Junichi Kitagawa, DDS, PhD
Assistant Professor
Department of Physiology
School of Dentistry at Tokyo
Nippon Dental University
Tokyo, Japan

Tadashi Kusama
Professor
College of Pharmacy, Nihon University
Chiba, Japan

Koichi Iwata
Professor
Department of Physiology
Nihon University School of Dentistry
Tokyo, Japan

Correspondence to:
Dr Koichi Iwata
Department of Physiology
Nihon University School of Dentistry
1-8-13 Kandasurugadai, Chiyoda-ku
Tokyo, 101-8310, Japan
Fax: +81 3 3219 8341
E-mail: Iwata-k@dent.nihon-u.ac.jp

Aims: To elucidate the neuronal mechanisms underlying chronic pain of the temporomandibular joint (TMJ), expression of phosphorylated extracellular signal-regulated kinase (pERK) in the trigeminal spinal nucleus caudalis (Vc) was studied in rats with a chronically inflamed TMJ. ***Methods:*** *Complete Freund's adjuvant (CFA) was injected in the left TMJ region of rats anesthetized with pentobarbital (50 mg/kg intraperitoneally). Face temperature of the TMJ region was measured periodically after CFA injection. Two weeks after CFA injection, passive jaw movement with 4-, 6-, and 15-mm distances was carried out in inflamed and naive rats for 5, 15, and 30 minutes. pERK expression was studied in the medulla and upper cervical cord after passive jaw movement.* ***Results:*** *Face temperature was significantly increased 2 days after CFA injection and returned to the preoperative level 7 days later. The pERK-like immunoreactive (LI) cells were observed in the dorsal portion of the rostral Vc in inflamed rats after passive jaw movement, and a small number of pERK-LI cells were observed in naive rats after passive jaw movement. No pERK-LI cells were observed in the TMJ of inflamed rats without jaw movement. The number of pERK-LI cells increased following increases in the jaw-movement distance and duration.* ***Conclusion:*** *These findings suggest that the dorsal portion of the rostral Vc may be involved in mediating chronic pain following TMJ inflammation and that the intracellular ERK cascade may be involved.* J OROFAC PAIN 2007; 21:225–231

Key words: chronic inflammation, extracellular signal-regulated kinase, jaw movement, temporomandibular joint, trigeminal spinal nucleus

Acute inflammation of the temporomandibular joint (TMJ) region causes sensitization of C-fibers in the TMJ capsule as well as neurons in the trigeminal spinal nucleus caudalis (Vc; also termed the medullary dorsal horn).[1–3] However, little is known about the neuronal mechanisms underlying chronic TMJ pain following peripheral inflammation.

The extracellular signal-regulated kinase (ERK) is 1 of the mitogen-activated protein kinases activated by calcium influx in dorsal root ganglion (DRG) and dorsal horn (DH) neurons.[4–7] It has been reported that C-fiber but not A-fiber stimulation induces phosphorylated ERK (pERK) expression in DH neurons.[5] It has been also reported that pERK expression peaks in the DRG and in DH neurons within 10 minutes after noxious stimulation.[4,7,8] Recently, Shimizu et al reported that pERK-LI cells are expressed in Vc within 10 minutes following capsaicin stimulation of the tooth pulp.[8] These data suggest that pERK is a potential marker of the excitation of DH neurons following noxious stimulation.

Thus, it was decided to analyze the change in pERK expression following jaw movement in rats with chronic TMJ inflammation in order to elucidate the neuronal mechanisms underlying chronic TMJ pain.

Materials and Methods

Lateral face temperature measurement (inflamed rats: n = 5, naive rats: n = 5), histologic analysis of the TMJ (2 days after injection of complete Freund's adjuvant [CFA]: n = 5; 14 days after CFA injection: n = 5), and pERK immunohistochemistry (inflamed rats: n = 45; naive rats: n = 45) were performed on male Sprague-Dawley rats (250 to 365 g).

The study was approved by the Animal Experimentation Committee at Nihon University School of Dentistry. The animals were treated according to the guidelines of the International Association for the Study of Pain.[9]

CFA Injection into the TMJ Region and Measurement of the Lateral Face Temperature

Rats were anesthetized with sodium pentobarbital (50 mg/kg, intraperitoneally). The inflammatory agent CFA was suspended in an oil-saline (1:1) emulsion, and a volume of 0.05 mL was injected into the left TMJ region through the facial skin with a 27-gauge needle under an optical microscope. One day later, rats were anesthetized, and the face temperature on the ipsilateral and contralateral sides was measured by a computer-assisted infrared thermograph (Thermo tracer TH3100ME, NEC-SANEI).

Passive Jaw Movement

Fourteen days after CFA injection, rats were anesthetized with sodium pentobarbital (50 mg/kg intraperitoneally) and placed on a flat plate. The gingiva around the mandibular incisors was locally anesthetized with 2% lidocaine. The hook of an electrically controlled vibrator was then placed on the gingiva around the mandibular incisors. Passive jaw movement was applied at 1 Hz (distance: 4 mm, 6 mm, and 15 mm; duration: 5 minutes, 15 minutes, and 30 minutes, n = 5 in each group). Passive jaw movement was also applied to naive rats (n = 5 in each group).

pERK Immunohistochemistry

Rats were perfused through the aorta with 200 mL 0.9% saline followed by 500 mL 4% paraformaldehyde in 0.1 mol/L phosphate buffer (PBS, pH 7.4) 5 minutes after passive jaw movement. Sections 30 μm wide were cut from the brainstem, and every fourth section was collected in PBS. Since a detailed pERK immunohistochemical procedure was reported previously,[8] the procedure is only briefly described here. Free-floating tissue sections were incubated in rabbit anti-Phospho-p44/42 MAP kinase antibody (1:1000, Cell Signaling Technology) and biotinylated goat anti-rabbit IgG (1:600; Vector Labs). The pERK-like immunoreactive (LI) cells were visualized using 0.035% 3,3'-diaminobenzidine-tetra HCl (DAB, Sigma).

Under a light microscope, the pERK-LI cells were drawn using a camera lucida drawing tube. The number of pERK-LI cells was counted from every eighth section. The total number of pERK-LI cells from 3 of these sections was calculated, and the mean number of pERK-LI cells (per section) was obtained for each rat.

Statistical Analysis

Statistical analysis was performed using analysis of variance (ANOVA) followed by a Fisher protected least significant difference (LSD) test, a Newman-Keuls test, a Dunnett test, or a Scheffé test. A Student t test or Welch's t test was also used as appropriate. Differences were considered significant at $P < .05$. Results are presented as means ± standard error of the mean (SEM).

Results

Face Temperature and TMJ Inflammation

The face temperature was significantly increased on the ipsilateral side compared to the contralateral side 2 days after CFA injection into the left TMJ and gradually decreased thereafter (Figs 1a and 1b). High-temperature areas were widely distributed over the whole lateral face, sometimes extending to the neck region (Fig 1a). The accumulation of a large number of inflammation-related cells, such as neutrophils and macrophages, was observed 2 days after CFA injection (Fig 2a). Many inflammation-related cells were packed in the space between the condylar head and capsule. However, no inflammation-related cells were observed at 14 days after CFA injection (Fig 2b).

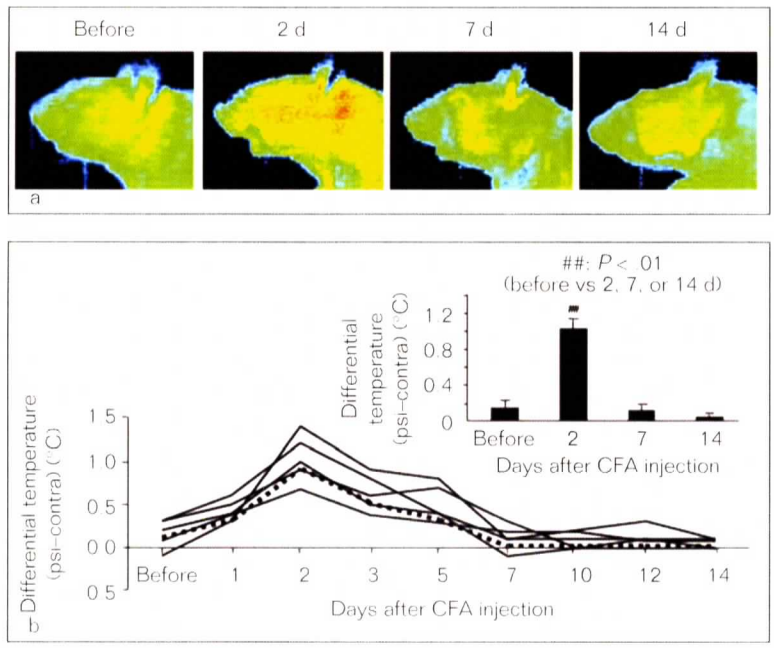

Fig 1 Change in face temperature following CFA injection into the left TMJ. *(a)* Typical example of the lateral face temperature following CFA injection. *(b)* Time-course of change in face temperature. The inset graph indicates the mean temperature difference between the ipsilateral and contralateral sides before and 2, 7, and 14 days after CFA injection. Dotted line in *b* indicates median face temperature.

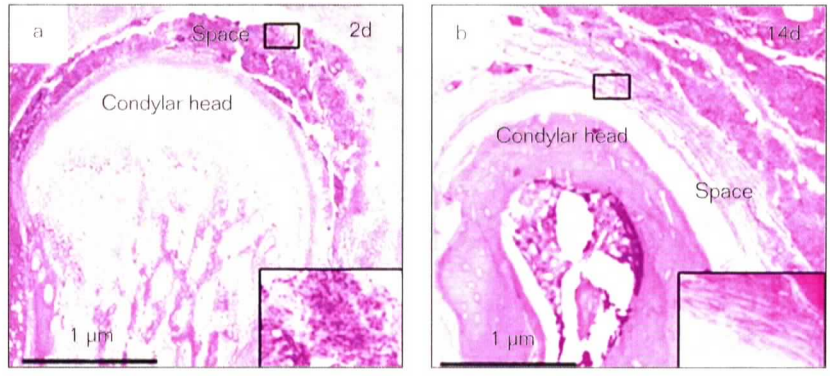

Fig 2 The TMJ capsule *(a)* 2 days and *(b)* 14 days after CFA injection into the left TMJ region. Insets are high-magnification photomicrographs of the areas indicated by the smaller squares.

Modulation of pERK Expression Following Change in Distance and Duration of Jaw Movement

A large number of pERK-LI cells were expressed in the superficial laminae of the dorsal portion of the ipsilateral Vc following 15 mm of passive jaw movement for 15 minutes at 14 days after TMJ CFA injection, as illustrated in Figs 3a to 3c. The pERK-LI cells were ipsilaterally dominant. pERK-LI cells were observed on the side contralateral to the CFA injection as well (Fig 3d). A small number of pERK-LI cells were expressed bilaterally in the Vc following 15 mm of passive jaw movement for 15 minutes in the rats without CFA (Figs 3e and 3f). However, no pERK-LI cells were observed in the TMJ-inflamed rats without jaw movement, as illustrated in Fig 3g.

The rostro-caudal distribution of pERK-LI cells for different jaw-movement distances and durations is illustrated in Figs 4a to 4c. A small number of pERK-LI cells were expressed following jaw movement in naive rats (Fig 4b). However, the number and the distribution area of pERK-LI cells were increased in the rostral Vc following jaw movements in the CFA-treated rats (Fig 4c). The increase in the number and distribution area of pERK-LI cells was predominantly seen on the side ipsilateral to the CFA injection site, but slight change was observed on the contralateral side.

The relationship between the mean number of pERK-LI cells and jaw movement duration and distance is illustrated in Figs 4d and 4e. More pERK-LI cells were expressed following 15 and 30 minutes of jaw movement with 15 mm of jaw movement than with 4 mm of jaw movement on

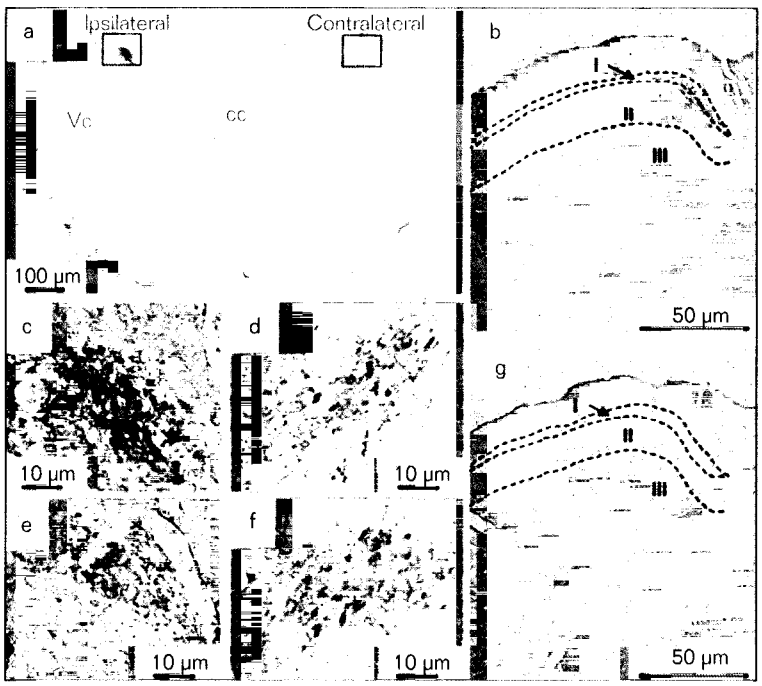

Fig 3 pERK-LI cells in Vc. *(a)* Vc at low magnification following 15 mm of jaw movement for 15 minutes at 14 days after CFA injection into the left TMJ. *(b and c)* The ipsilateral Vc at high magnification following 15 mm of jaw movement for 15 minutes at 14 days after CFA injection into the left TMJ. *(d)* The contralateral Vc at high magnification following 15 mm of jaw movement for 15 minutes *(e and f)* The ipsilateral and contralateral Vc, respectively, at high magnification in a naive rat following 15 mm of jaw movement for 15 minutes. *(g)* The ipsilateral Vc at high magnification in a CFA-injected rat without jaw movement. I = lamina I, II = lamina II, III = lamina III.

the side ipsilateral to CFA injection ($P < .01$). A stronger expression of pERK-LI cells was observed at the 15-mm distance compared to 4 mm for 30 minutes of jaw movement. The number of pERK-LI cells was also significantly larger in rats, with longer duration of jaw movement on the ipsilateral side to CFA injection after 15 mm of jaw movement (Fig 4d). However, no obvious increase in the number of pERK-LI cells was observed on the contralateral side (Fig 4e).

Discussion

An increase in the face temperature occurred after CFA injection into the TMJ region. It is well known that a change in skin temperature of an inflamed region is a good indicator of inflammation.[10,11] Face temperature was maximal 2 days after the CFA injection. Evans' blue extravasation was measured in previous studies to verify the extent of inflammation.[12,13] It has been reported that Evans' blue extravasation in the TMJ capsule is significantly increased 2 to 3 days after TMJ CFA injection. These findings suggest that acute inflammation became maximal 2 to 3 days after CFA injection. No increase in face temperature was noted 14 days after CFA injection, suggesting that the TMJ inflammation was in a chronic state at this period.

It has been reported that CFA injection into the TMJ region induces a variety of changes in Vc neuronal activity.[1] Three days after CFA injection, receptive field size was significantly expanded, and background activity and heat-evoked responses were significantly increased. These changes in neuronal activity are thought to result from central sensitization of the Vc nociceptive neurons. The Vc nociceptive neurons modulated by CFA injection into the TMJ region were distributed in the middle portion of the Vc. On the other hand, jaw movement caused a strong expression of pERK-LI cells in the dorsal portion of rostral Vc following CFA injection into the TMJ region in the present study. It is likely that many rostral Vc neurons are recruited during jaw movement in rats with chronic TMJ inflammation. In a single-unit recording study, the limited location of the cells responding to TMJ CFA-induced inflammation (the middle part of Vc) was probably due to the limited sampling in those experiments, and it is likely that recordings in the dorsomedial part of the rostral Vc would also have revealed evidence of hyperexcitability.[1] In the present study, it was observed that the ERK phosphorylation was enhanced following an increase in the duration and distance of jaw movement in the rats with chronic TMJ inflammation. A slight increase in pERK-LI cells was also observed in the noninflamed rats after

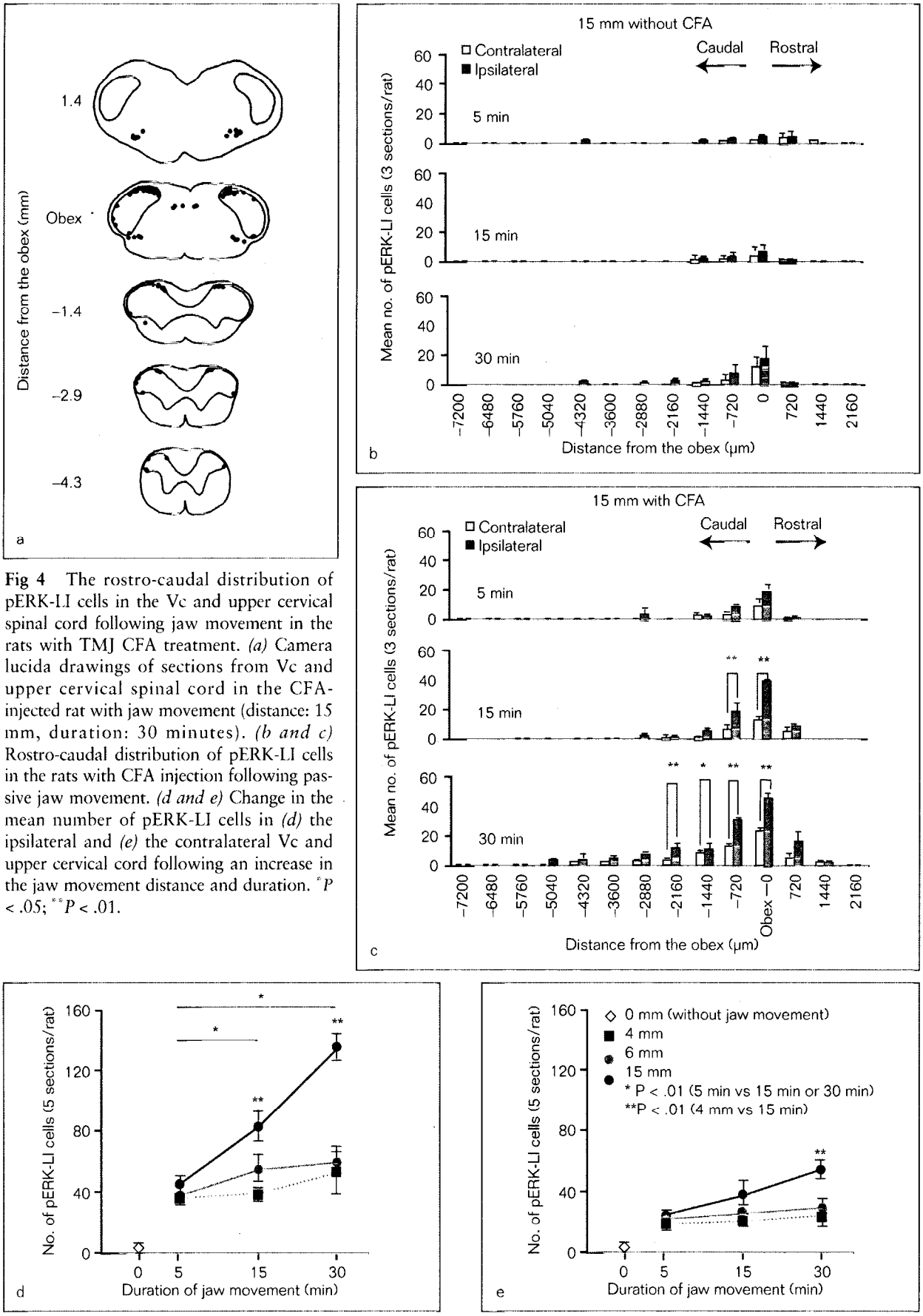

Fig 4 The rostro-caudal distribution of pERK-LI cells in the Vc and upper cervical spinal cord following jaw movement in the rats with TMJ CFA treatment. *(a)* Camera lucida drawings of sections from Vc and upper cervical spinal cord in the CFA-injected rat with jaw movement (distance: 15 mm, duration: 30 minutes). *(b and c)* Rostro-caudal distribution of pERK-LI cells in the rats with CFA injection following passive jaw movement. *(d and e)* Change in the mean number of pERK-LI cells in *(d)* the ipsilateral and *(e)* the contralateral Vc and upper cervical cord following an increase in the jaw movement distance and duration. $^{*}P < .05$; $^{**}P < .01$.

jaw movement. It is very important that pERK was expressed only after jaw movement; this indicates that ERK was not phosphorylated under chronic TMJ inflammation unless mechanical stimulation was also present. It has been reported that Fos-positive neurons are expressed in the Vc and upper cervical cord after CFA injection into the TMJ region of rats with and without jaw movement.[13–16] This suggests that the Fos-LI cells are expressed as the result of an increase in spontaneous and evoked activities following TMJ inflammation. On the other hand, ERK phosphorylation occurs as the result of evoked activity but not spontaneous activity. This suggests that the intracellular ERK cascade is involved in the dynamic responses of nociceptive neurons in Vc.

It has been reported that many Fos-LI cells are expressed in the Vi/Vc, Vc, and the upper cervical cord following CFA injection into the TMJ region.[13–16] A large number of pERK-LI cells were found in the present study in the dorsal portion of the rostral Vc and overlapped with the areas where Fos protein-LI cells have been reported to be expressed after TMJ inflammation. However, significant expression of pERK-LI cells in the upper cervical spinal cord in the CFA-treated rats following passive jaw movement was not observed. It has been reported that Fos protein is expressed in spinal dorsal horn neurons 0.5 to 1.0 hours following noxious stimulation of the skin, whereas pERK is expressed within 10 minutes. The time-course difference in expression between pERK and Fos protein may reflect the distribution difference of positive neurons in the Vi/Vc zone and upper cervical spinal cord. Furthermore, there are a number of intracellular transduction pathways that produce Fos protein. The ERK phosphorylation cascade is thought to be 1 of the pathways for Fos production. It is likely that the different intracellular transduction cascades for Fos production and ERK phosphorylation are involved in the distribution differences between pERK and Fos-positive neurons.

It is probable that the pERK expression in the rostral Vc neurons is an earlier event in TMJ nociception compared to that of Fos expression. Together with previous Fos studies, the present ERK study strongly suggests that the Vi/Vc neurons, rostral Vc neurons, and the upper cervical cord neurons are involved in chronic TMJ pain.

Conclusions

A large number of phosphorylated extracellular signal-regulated kinase-like immunoreactive cells were observed in lamina I of the dorsal portion of the rostral Vc of TMJ-inflamed rats after passive jaw movement. The number of pERK-LI cells gradually increased following increases in jaw movement, distance, and duration. These findings suggest that neurons in the dorsal portion of the rostral Vc may be involved in chronic TMJ pain following TMJ inflammation through an intracellular MAP kinase signal transduction cascade that involves ERK phosphorylation.

Acknowledgments

This study was supported in part by research grants from the Sato and Uemura Funds; a grant from Dental Research Center, Nihon University School of Dentistry; a multidisciplinary research grant and an individual research grant from Nihon University; a grant from the Ministry of Education, Culture, Sports, Science, and Technology to promote multidisciplinary research projects; and a grant from the Ministry of Education, Culture, Sports, Science, and Technology to promote multidisciplinary research on "Brain Mechanisms for Cognition, Memory and Behavior" at Nihon University. The authors thank Dr D. A. Thomas for correcting the English usage.

References

1. Iwata K, Tashiro A, Tsuboi Y, et al. Medullary dorsal horn neuronal activity in rats with persistent temporomandibular joint and perioral inflammation. J Neurophysiol 1999;82:1244–1253.
2. Bereiter DA, Bereiter DF, Ramos M. Vagotomy prevents morphine-induced reduction in Fos-like immunoreactivity in trigeminal spinal nucleus produced after TMJ injury in a sex-dependent manner. Pain 2002;96:205–213.
3. Bereiter DA, Okamoto K, Bereiter DF. Effect of persistent monoarthritis of the temporomandibular joint region on acute mustard oil-induced excitation of trigeminal subnucleus caudalis neurons in male and female rats. Pain 2005;117:58–67.
4. Dai Y, Iwata K, Fukuoka T, et al. Phosphorylation of extracellular signal-regulated kinase in primary afferent neurons by noxious stimuli and its involvement in peripheral sensitization. J Neurosci 2002;22:7737–7745.
5. Ji RR, Baba H, Brenner GJ, Woolf CJ. Nociceptive-specific activation of ERK in spinal neurons contributes to pain hypersensitivity. Nat Neurosci 1999;2:1114–1119.
6. Kawasaki Y, Kohno T, Zhuang ZY, et al. Ionotropic and metabotropic receptors, protein kinase A, protein kinase C, and Src contribute to c-fiber-induced ERK activation and cAMP response element-binding protein phosphorylation in dorsal horn neurons, leading to central sensitization. J Neurosci 2004;24:8310–8321.

7. Liu Y, Obata K, Yamanaka H, et al. Activation of extracellular signal-regulated protein kinase in dorsal horn neurons in the rat neuropathic intermittent claudication model. Pain 2004;109:64–72.
8. Shimizu K, Asano M, Kitagawa J, et al. Phosphorylation of extracellular signal-regulated kinase in medullary and upper cervical cord neurons following noxious tooth pulp stimulation. Brain Res 2006;1072:99–109.
9. Zimmerman M. Ethical guidelines for investigation of experimental pain in conscious animals. Pain 1983;16:109–110.
10. Kitagawa J, Kanda K, Sugiura M, et al. Effect of chronic inflammation on dorsal horn nociceptive neurons in aged rats. J Neurophysiol 2005;93:3594–3604.
11. Koyama N, Hirata K, Hori K, et al. Computer-assisted infrared thermographic study of axon reflex induced by intradermal melittin. Pain 2000;84:133–139.
12. Ogawa A, Ren K, Tsuboi Y, Morimoto T, Sato T, Iwata K. A new model of experimental parotitis in rats and its implication for trigeminal nociception. Exp Brain Res 2003;152:307–316.
13. Zhou Q, Imbe H, Dubner R, Ren K. Persistent Fos protein expression after orofacial deep or cutaneous tissue inflammation in rats: Implications for persistent orofacial pain. J Comp Neurol 1999;412:276–291.
14. Sessle BJ, Greenwood LF. Inputs to trigeminal brain stem neurons from facial, oral, tooth and pharyngolaryngeal tissues. I. Responses to innocuous and noxious stimuli. Brain Res 1976;117:211–226.
15. Hathaway CB, Hu JW, Bereiter DA. Distribution of Fos-like immunoreactivity in the caudal brainstem of the rat following noxious chemical stimulation of the temporomandibular joint. J Comp Neurol 1995;356:444–456.
16. Bereiter DA, Cioffi JL, Bereiter DF, et al. Local blockade of integrins in the temporomandibular joint region reduces Fos-positive neurons in trigeminal subnucleus caudalis of female rats produced by jaw movement. Pain 2006;125:65–73.

available at www.sciencedirect.com

SCIENCE DIRECT®

www.elsevier.com/locate/brainres

BRAIN RESEARCH

Research Report

Phosphorylation of Extracellular Signal-Regulated Kinase in medullary and upper cervical cord neurons following noxious tooth pulp stimulation

Kohei Shimizu[a], *Masatake Asano*[b], *Junichi Kitagawa*[c,e], *Bunnai Ogiso*[a,d], *Ke Ren*[f], *Hidero Oki*[g], *Mitsuhiko Matsumoto*[g], *Koichi Iwata*[c,e,h,*]

[a]*Department of Endodontics, School of Dentistry, Nihon University, 1-8-13 Kandasurugadai, Chiyoda-ku, Tokyo 101-8310, Japan*
[b]*Department of Pathology, School of Dentistry, Nihon University, 1-8-13 Kandasurugadai, Chiyoda-ku, Tokyo 101-8310, Japan*
[c]*Department of Physiology, School of Dentistry, Nihon University, 1-8-13 Kandasurugadai, Chiyoda-ku, Tokyo 101-8310, Japan*
[d]*Division of Advanced Dental Treatment, Dental Research Center, Nihon University School of Dentistry, Tokyo 101-8310, Japan*
[e]*Division of Functional Morphology, Dental Research Center, Nihon University School of Dentistry, Tokyo 101-8310, Japan*
[f]*Department of Biomedical Sciences, University of Maryland Dental School, Baltimore, MD 21201, USA*
[g]*Department of Oral and Maxillofacial Surgery, School of Dentistry, Nihon University, 1-8-13 Kandasurugadai, Chiyoda-ku, Tokyo 101-8310, Japan*
[h]*Division of Applied System Neuroscience Advanced Medical Research Center, Nihon University Graduate School of Medical Science, 30-1 Ohyaguchi-Kamimachi Itabashi, Tokyo 173-8610, Japan*

ARTICLE INFO

Article history:
Accepted 5 December 2005
Available online 25 January 2006

Keywords:
MAPK
ERK
Fos
Tooth pulp
Capsaicin
Spinal trigeminal nucleus

ABSTRACT

The phosphorylated Extracellular Signal-regulated Kinase (pERK) and Fos expression and masticatory muscle activity were analyzed in rats with capsaicin-induced acute inflammation of the tooth pulp in order to clarify the role of the spinal trigeminal nucleus and upper cervical spinal cord in tooth pulp pain. Digastric and masseteric muscle activities were significantly increased following capsaicin injection into the molar tooth pulp but not after vehicle treatment. The pERK-like immunoreactive (LI) neurons were observed in the subnuclei interpolaris–caudalis transition (Vi/Vc) zone, the paratrigeminal nucleus (Pa5) and the superficial laminae of the caudal Vc/C2 zone. The pERK expression was detected as early as 2 min and peaked at 5 min after capsaicin or vehicle injection. The pERK expression in the Vi/Vc zone and Pa5 was bilateral, whereas it was predominantly ipsilateral in the caudal Vc/C2 zone. The capsaicin treatment of the whisker pad produced pERK expression in the rostro-caudal middle portion of the ipsilateral Vc, but small number of pERK-LI cells were observed after vehicle treatment. The pERK expression was similar in the Vi/Vc zone following capsaicin injection into the upper or lower molar tooth pulp, whereas the pERK expression was in the lateral portion of the caudal Vc/C2 zone after upper molar injection and restricted to the medial portion of the Vc/C2 zone after the lower molar capsaicin. These data were confirmed with Western blots. There were differences in the distribution of Fos protein-like immunoreactive (LI) cells and pERK-LI cells following tooth pulp stimulation. After capsaicin application into the upper molar tooth pulp, no pERK-LI cells were observed

* *Corresponding author*. Fax: +81 3 3219 8341.
E-mail address: iwata-k@dent.nihon-u.ac.jp (K. Iwata).

doi:10.1016/j.brainres.2005.12.040

in the ventral part of the Vi/Vc zone, whereas many Fos protein-LI cells were expressed in this region. The difference in the distribution pattern of pERK- and Fos protein-LI cells in the Vi/Vc zone suggests their differential temporal expression profiles after capsaicin. The present findings suggest that tooth-pulp-driven neurons in the spinal trigeminal nucleus are involved in tooth pulp pain through activation of the intracellular signal transduction pathway that involves earlier ERK phosphorylation and subsequent Fos expression.

1. Introduction

The Extracellular-Signal-regulated Kinase (ERK) is one of the mitogen-activated protein kinases (MAPKs) activated by calcium influx in the dorsal root ganglion (DRG) and dorsal horn (DH) neurons (Ji et al., 1999, 2002; Kawasaki et al., 2004). A variety of peripheral stimuli activate MAPKs pathways (Dai et al., 2002; Ji et al., 2002; Liu et al., 2004; Obata et al., 2004a,b). Phosphorylation of ERK (pERK) is known to be induced as a result of neuronal activation. Specifically, it has been reported that C-fiber stimulation induces pERK expression in the DH neurons but not low threshold A-fiber stimulation (Ji et al., 1999). It has been also reported that the pERK expression peaked in DRG and DH neurons within 10 min after noxious stimulation (Dai et al., 2002; Liu et al., 2004; Wang et al., 2004). The pERK expression in DH neurons was also modulated by NMDA receptor antagonist (Ji et al., 1999, 2002). These data suggest that pERK is a potential marker of the excitability of DH nociceptive neurons following noxious stimulation of peripheral structures, which occurs at the early period after stimulation. The digastric and masseteric muscles are known to be activated by the noxious stimulation of the tooth pulp as well as a variety of trigeminal structures (Park et al., 2001; Sunakawa et al., 1999). The EMG activity was reported to be elicited just after noxious stimulation of the tooth pulp and lasting for a while (Sunakawa et al., 1999). The time-course of the EMG activity was similar to that of pERK expression. Therefore, it is very convenient to compare the EMG activity and pERK expression in order to study the change in neuronal activity after trigeminal noxious stimulation.

A large number of nociceptive neurons in the subnucleus caudalis (Vc) of the spinal trigeminal nucleus (Sp5) are responsive to a variety of stimuli applied to the tooth pulp (Chattipakorn et al., 2001, 2002; Hu and Sessle, 1984; Hu et al., 1981; Iwata et al., 1998; Oakden and Boissonade, 1998; Sessle, 1987; Sessle and Greenwood, 1976; Sessle et al., 1986; Sugimoto et al., 1998). The Vc has been known as an important nucleus relaying tooth pulp sensory information to the higher central nervous system (CNS). Electrical stimulation of the tooth pulp induces a large number of Fos protein-LI cells in the transition zone between the subnuclei interpolaris and caudalis (Vi/Vc zone) and the caudal Vc and the upper cervical cord (Vc/C2 zone). These two zones play an important role in conveying sensory information of the tooth pulp (Iwata et al., 1998). Electrophysiological studies have reported that most Vc neurons responsive to tooth pulp stimulation (tooth-pulp-driven neurons) receive noxious and/or non-noxious cutaneous inputs from the jaw and orofacial regions (Sessle, 1987; Sessle and Greenwood, 1976; Sessle et al., 1986). Thus, tooth-pulp-driven neurons in the Vc have functional roles in relaying trigeminal cutaneous information as well as tooth pulp input. It is still unknown how these two CNS regions are involved in processing tooth pulp noxious information. In the present study, we focused on these two regions to clarify the functional differences of tooth-pulp-driven neurons activated by capsaicin injection. It has been known that Fos is a marker of dorsal horn neuronal activation following peripheral noxious stimulation. However, the Fos analysis is not adequate to study the event occurring at the early time period after noxious stimulation of peripheral structures. A variety of chemicals are known as the possible peripheral irritants to activate peripheral nociceptors. However, capsaicin is one of the irritants whose peripheral mechanism is well known, capsaicin is dominantly involved in an acute activation of C-fiber afferents (Caterina et al., 1997). Thus, the pERK expression in the Sp5 and upper cervical cord was analyzed in rats receiving capsaicin treatment of the tooth pulp in order to clarify the distribution pattern of active neurons in the medulla and the upper cervical cord at the early period after capsaicin stimulation, and the results compared to that of Fos expression and that following cutaneous capsaicin injection into the region of the whisker pad.

2. Results

The digastric and masseteric electromyographic (EMG) muscle activities were significantly increased following capsaicin injection into the upper molar tooth pulp as illustrated in Fig. 1. The EMG activities of these two muscles were simultaneously increased and lasted for about 3–5 min after capsaicin injection. In general, the capsaicin-evoked digastric EMG activity was much larger and longer lasting as compared to the masseteric EMG (Fig. 1B). There was no change in EMG activities following the vehicle injection into the molar tooth pulp (Fig. 1C).

The pERK-like immunoreactive (LI) neurons were observed in the dorsal portion of the Vi/Vc zone and Pa5 bilaterally 5 min after capsaicin injection into the upper molar (Figs. 2A–E and 3). In the caudal Vc/C2 zone, pERK-LI neurons were mainly found in the lateral portion of the ipsilateral superficial laminae, and there were only a few pERK-LI cells in the contralateral Vc/C2 zone (Figs. 2C and F). The increase in pERK activity in the Vi/Vc zone (Pa5 was included in this region) and Vc/C2 zone was verified with Western blot analysis following capsaicin injection into the tooth pulp as compared to vehicle-treated rats (Figs. 2Ga and b). The pERK and total ERK immuno-products exhibited as two 42 kDa and 44 kDa bands on Western blot (Fig. 2G). The pERK expression was different between the Vi/Vc zone + Pa5 and Vc/C2 zone. The 42 kDa band was expressed in the Vi/Vc

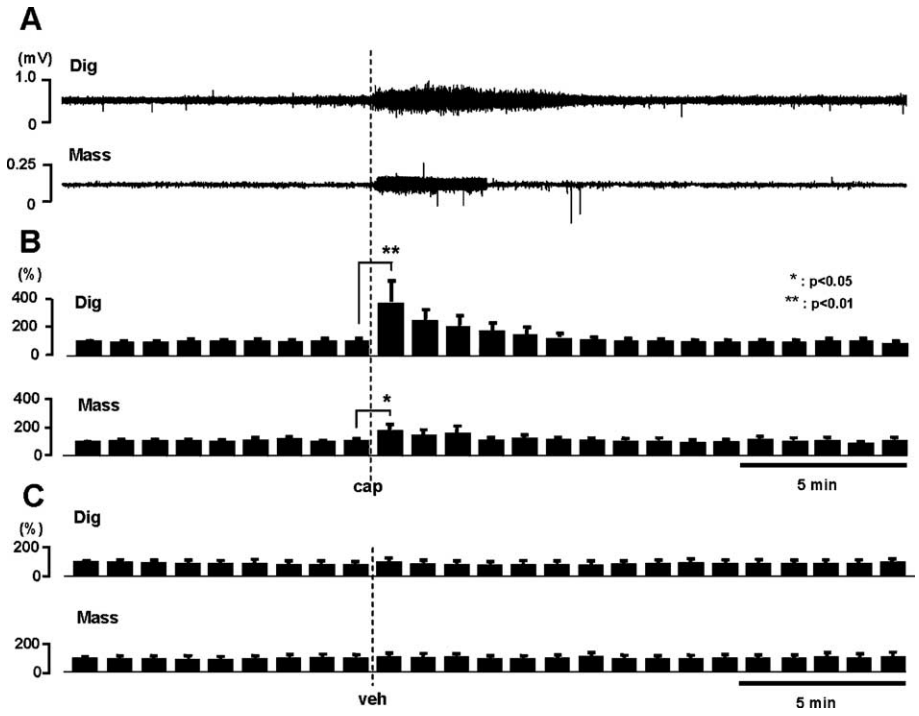

Fig. 1 – Digastric and masseter muscle EMG activities ipsilateral to capsaicin or vehicle injection. (A) Typical responses of EMG activities recorded from digastric (Dig) and masseter (Mass) muscles following capsaicin injection into the upper molar tooth pulp. (B) Percent change in Dig and Mass muscle activities following capsaicin injection into the upper molar tooth pulp (n = 5). (C) Percent change in Dig and Mass muscle activities following vehicle injection into the upper molar tooth pulp. cap: capsaicin, veh: vehicle (LSD test).

zone + Pa5 bilaterally, whereas it was only observed in the ipsilateral Vc (Fig. 2G). This is consistent with the immunohistochemistry results (Figs. 2A–F). There were no differences in the total ERK expression between the Vi/Vc zone + Pa5 and Vc/C2 zones and also no differences between capsaicin and vehicle-treated rats.

The camera-lucida drawings of pERK-LI cells are illustrated in Fig. 3. The pERK-LI cells were basically restricted to the nucleus and are represented as small dots in each section. Following capsaicin injection into the upper molar, a large number of pERK-LI cells were expressed in the dorsomedial portion of the Vi/Vc zone bilaterally. On the other hand, pERK-LI cells showed relatively wider distribution in the Vi/Vc zone following lower molar injection. We also observed a large number of pERK-LI cells in the rostro-caudally middle portion of the ipsilateral Vc following capsaicin injection into the whisker pad region. A few pERK-LI cells were expressed in the contralateral Vc after whisker pad injection. In the Vc/C2 zone, the distribution patterns of pERK-LI cells were different between the injections into the upper and lower molars and whisker pad. The pERK-LI cells were restricted in the lateral portion of the ipsilateral Vc/C2 zone after capsaicin injection into the upper molar. On the other hand, pERK-LI cells were distributed in the medial half of the ipsilateral Vc/C2 zone following lower molar injection. Only a few pERK-LI cells were observed in the ipsilateral Vc/C2 zone following capsaicin injection into the whisker pad region. In the Pa5, a small number of pERK-LI cells were expressed bilaterally after capsaicin injection into the molar tooth pulps. The pERK-LI cells in the rostral Pa5 were significantly larger in the ipsilateral side as compared to contralateral side (Fig. 4A). However, distribution pattern of pERK-LI cells in the Pa5 through rostro-caudal extension was similar between ipsilateral and contralateral sides. Almost no pERK-LI cells were expressed in the contralateral Vc following whisker pad capsaicin injection. There were also pERK-LI cells in the Vi/Vc zone, Pa5 and Vc/C2 zone following vehicle injection into the molar tooth pulps. Although the distribution patterns of pERK-LI cells after vehicle injection into the tooth pulp were similar to that after capsaicin treatment, there was a significant difference in the number of pERK-LI cells (Fig. 4).

The rostro-caudal distribution of pERK-LI cells following capsaicin or vehicle treatment of the tooth pulp is summarized in Fig. 4. Following capsaicin injection into the upper molar tooth pulp, the pERK-LI cells were expressed with two peaks along the rostro-caudal extent of the Vc. One peak was in the Vi/Vc zone about 0–0.7 mm caudal to the obex, and the other peak was in the Vc/C2 zone at about 6.5 mm caudal to the obex. There were no distribution differences in pERK-LI cells between the ipsilateral and contralateral sides of the Vi/Vc zone following capsaicin injection into the upper molar tooth pulp (Fig. 4A, $p > 0.05$, Student's or Welch's test). On the other hand, the number of pERK-LI cells was significantly larger in the ipsilateral side than that

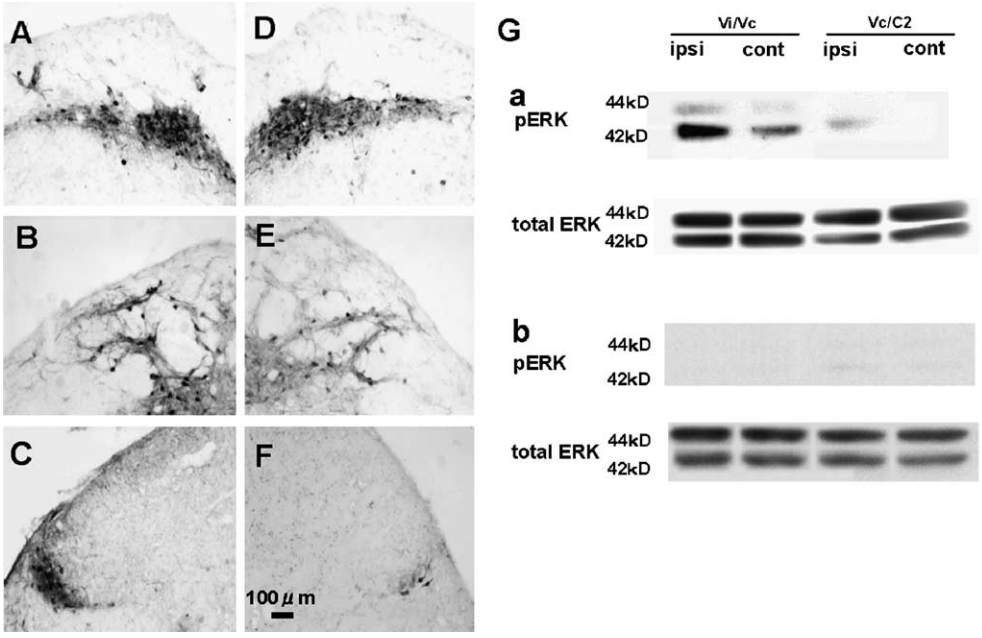

Fig. 2 – Capsaicin-induced pERK-LI cells in the medulla and upper cervical spinal cord. (A) Ipsilateral Vi/Vc zone. (B) Ipsilateral Pa5. (C) Ipsilateral Vc/C2 zone. (D) Contralateral Vi/Vc zone. (E) Contralateral Pa5. (F) Contralateral Vc/C2 zone. (G) Western blot illustrating the levels of pERK and total ERK in the Vi/Vc zone + Pa5 and Vc/C2 zone in the rat with capsaicin stimulation of the tooth pulp (a) and without capsaicin stimulation (b). Vc: trigeminal spinal nucleus caudalis, Pa5: paratrigeminal nucleus, C2: second cervical spinal cord. ipsi: ipsilateral, cont: contralateral.

of contralateral side in the Vc/C2 zone after capsaicin injection into the upper molar tooth pulp (Figs. 4A and C, $p < 0.05$, Student's or Welch's test). The pERK-LI cells were also seen bilaterally in the Pa5. A small number of pERK-LI cells were expressed in the Vi/Vc zone, Pa5 and Vc/C2 zone after vehicle injection into the tooth pulp, but the number of pERK-LI cells was significantly smaller as compared to that of the capsaicin-treated rats.

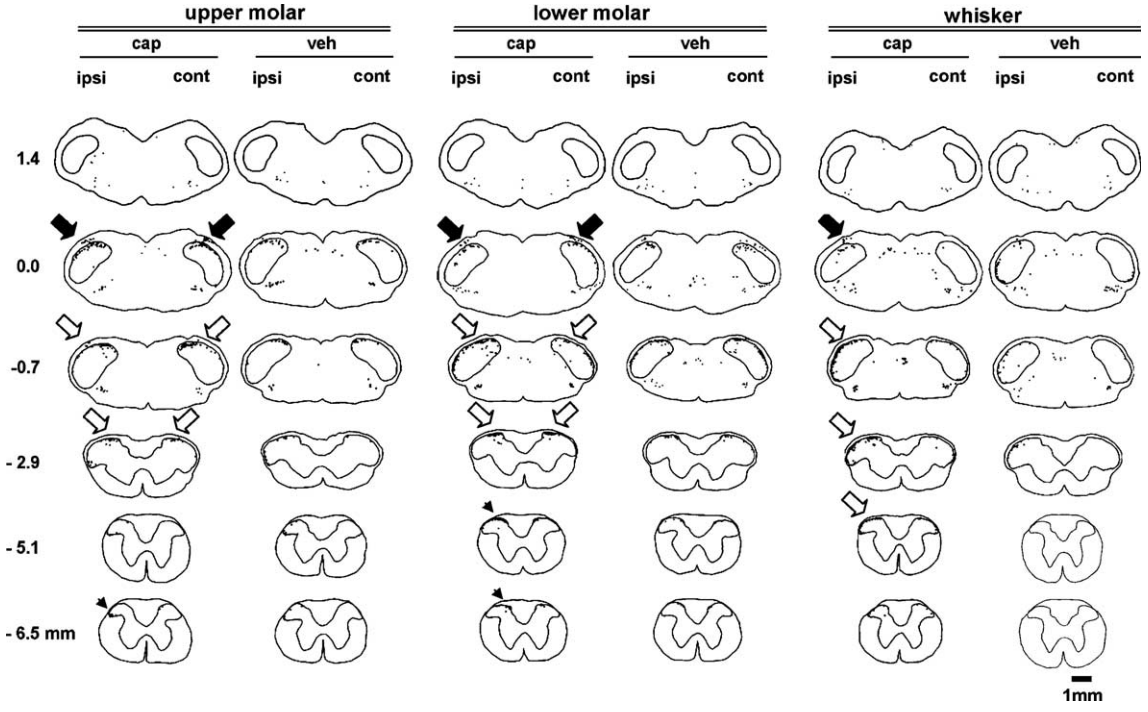

Fig. 3 – Camera-lucida drawings of pERK-LI cells in the medulla and upper cervical spinal cord following capsaicin injection into the tooth pulp or whisker pad region. Each dot indicates one pERK-LI cell. Solid arrows: Pa5 regions, open arrows: Vi/Vc zone, small arrows: Vc/C2 zones. The negative numbers on the left indicate the distance caudal to the obex.

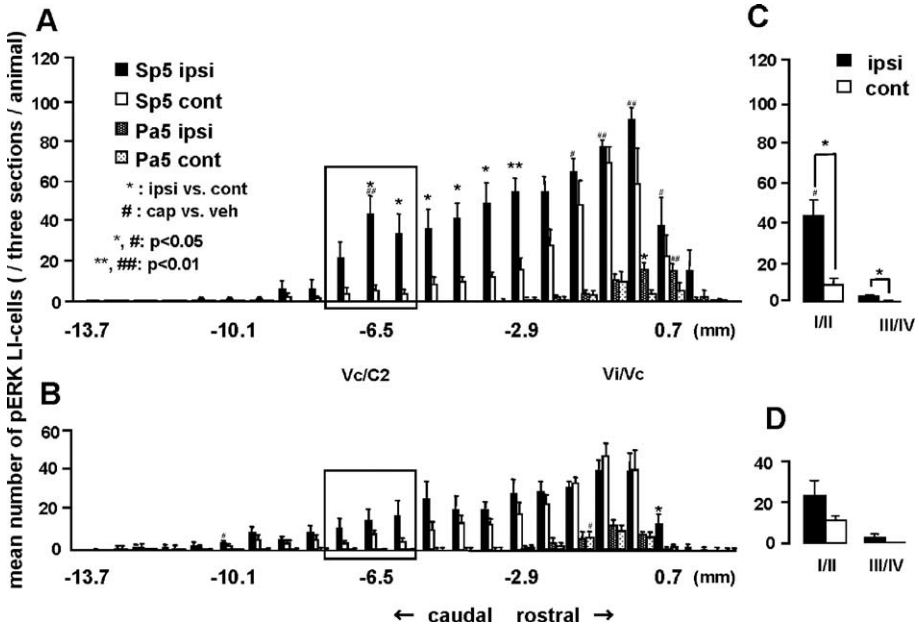

Fig. 4 – Rostro-caudal distribution of pERK-LI cells in the medulla and upper cervical spinal cord. The number of pERK-LI cells was plotted against the distance caudal the obex. (A) Data from the capsaicin-treated rats (n = 5). (B) Data from the vehicle-treated rats. (C) Laminar distribution of pERK-LI cells in the Vc/C2 zone of the capsaicin-treated rats. (D) Laminar distribution of pERK-LI cells in the Vc/C2 zone of the vehicle-injected rats. Sp5: spinal trigeminal nucleus (ipsi vs. cont: Student's or Welch's test, cap vs. veh: Newmann–Keuls test).

The time-course of the changes in pERK expression following capsaicin treatment of the upper molar tooth pulp is illustrated in Fig. 5. We observed significant increase in EMG activity within 5 min following capsaicin injection into the tooth pulp with similar time-course in pERK expression as illustrated in Figs. 1 and 5. The pERK expression started at 2 min and peaked at 5 min after capsaicin injection. After the 5 min time point, the number of pERK-LI cells gradually decreased and returned to the control level at 2 h after capsaicin injection (Fig. 5). The changes in the number of pERK-LI cells showed a similar time-courses in both sides of the Vi/Vc zone (Fig. 5A). The time-course of the change in the number of pERK-LI cells in the Pa5 following capsaicin treatment of the upper molar tooth pulp was similar to that of the Vi/Vc zone (Fig. 5B). The changes in the number of pERK-LI cells showed a similar time-course following capsaicin treatment of the tooth pulp in the ipsilateral Vc/C2 zone (Fig. 5C).

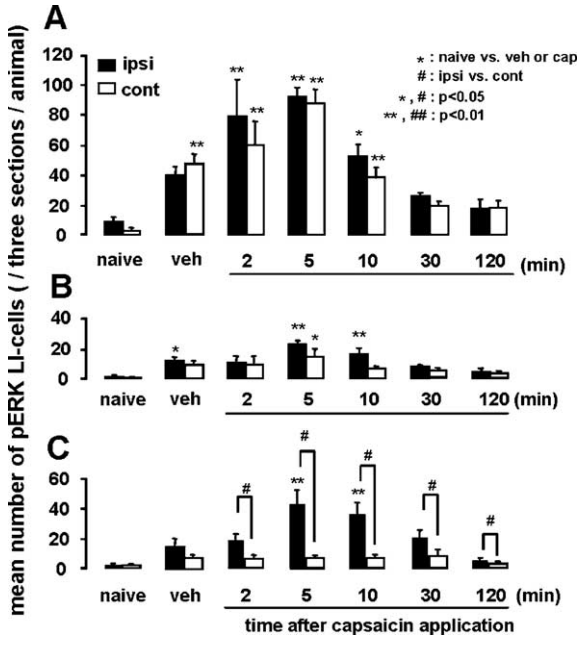

Fig. 5 – Time-course of the change in the number of pERK-LI cells in the Vi/Vc zone (A), Pa5 (B) and Vc/C2 zone (C) following capsaicin injection into the upper molar tooth pulp (n = 5 per time point). naive: rats without any stimulation, veh: rats with vehicle injection into the tooth pulp (naive vs. cap: Dunnett's test, ipsi vs. cont: Student's or Welch's test).

The comparison of distribution patterns of pERK-LI cells between the tooth pulp injection and whisker pad injection is illustrated in Fig. 6. Following capsaicin injection into the whisker pad region, a significantly larger number of pERK-LI cells were seen in the ipsilateral Vi/Vc zone and Vc/C2 zone as compared to the contralateral side (Fig. 6). On the other hand, the number of pERK-LI cells was not different between ipsilateral and contralateral sides in the Vi/Vc zone and ipsilateral dominant in the Vc/C2 zone after capsaicin treatment of the molar tooth pulp (Fig. 6). We also studied the comparison between pERK expression and Fos expression in the rats with capsaicin treatment of the upper tooth pulp.

A large number of Fos protein-LI cell were observed in the dorsal and ventral parts of the Vi/Vc zone and Pa5 bilaterally, and in the Vc/C2 zone with ipsilateral dominant 1 h after capsaicin treatment of the upper tooth pulp (Fig. 7). We could observe the significant expression of Fos protein-LI cells in the rats with vehicle treatment (Fig. 7B). The distribution difference in Fos protein- and pERK-LI cells was observed in

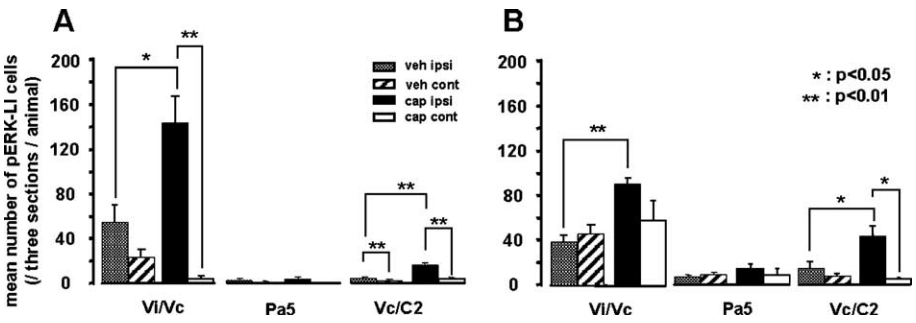

Fig. 6 – The number of pERK-LI cells in the Vi/Vc zone, Pa5 and Vc/C2 following capsaicin injection into the whisker pad (A) and the expression of pERK-LI cells in the rats with capsaicin injection into the upper molar tooth pulp (B). cap: capsaicin, veh: vehicle (ipsi vs. cont: Student's or Welch's test).

the ventral portion of the Vi/Vc zone as indicated by the arrows in Fig. 7B. No pERK-LI cells were expressed in the ventral portion of the Vi/Vc zone following tooth pulp capsaicin treatment (Fig. 3).

3. Discussion

Tooth pulp afferents project to the Sp5 and were somatotopically arranged in the Sp5 complex (Pertovaara et al., 1987; Sessle, 1987; Shigenaga et al., 1986, 1989). Tooth pulp afferents contain both high and low threshold nerve fibers (Jyvasjarvi and Kniffki, 1992; Narhi et al., 1992). It is well known that the sensory innervation of tooth pulp is very rich, and it consists almost purely of nociceptive Aδ- and C-fibers and of very scarce amount of fast conducting Aβ-fibers (Byers, 1984). The functional role of these pulpal Aβ-fibers is unclear, and, for example, they do not respond to non-noxious mechanical stimulation of the intact tooth (Narhi et al., 1992). More recent studies and detailed comparisons of the response characteristics of pulpal nociceptive Aδ- and Aβ-fibers indicated that they most likely belong to the same functional group (Byers and Narhi, 1999; Narhi et al., 1994).

Aδ and C-fibers in the tooth pulp are known to be involved in tooth pulp pain. Aδ-fibers in the tooth pulp are activated by a variety of natural stimuli applied to the tooth (Addy and Pearce, 1994). On the other hand, the tooth pulp C-fibers respond to the noxious stimulation of the pulp such as chemical and thermal stimuli (Narhi et al., 1992; Sessle, 1987). Aδ-fibers are involved in acute non-inflamed pain, whereas C-fibers are involved in tooth pulp inflamed pain. It is still unclear, however, how these two different types of tooth pulp afferents contribute to activation of CNS neurons that related to tooth pulp pain. Recent reports indicate that the Vi/Vc zone, Pa5 and upper cervical cord have differential roles in processing noxious information in the trigeminal system (Chattipakorn et al., 2001, 2002; Iwata et al., 1998, 2004). Fos expression is induced at about 1 h after noxious stimulation of

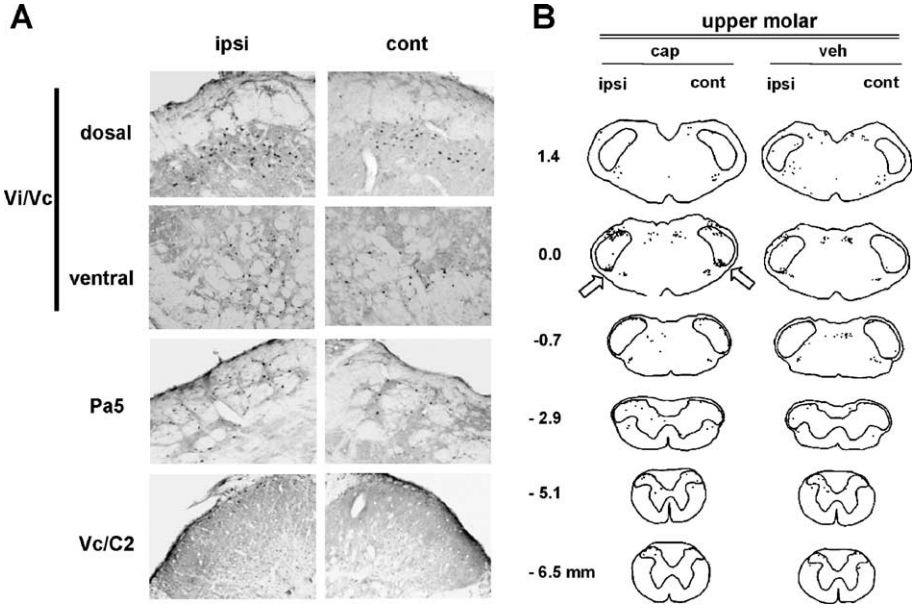

Fig. 7 – Fos expression in the Vi/Vc zone, Pa5 and Vc/C2 zone following capsaicin injection into the upper molar tooth pulp. (A) Photomicrographs of Fos protein-LI cells in the Vi/Vc zone, Pa5 and Vc/C2 zone. (B) Camera-lucida drawings of Fos protein-LI cells in the medulla and upper cervical spinal cord 1 h after capsaicin injection into the upper molar tooth pulp. Arrows indicate the ventral region of Vi/Vc zone.

peripheral structures (Tokunaga et al., 1995). On the other hand, pERK is expressed within 10 min following noxious peripheral stimulation (Ji et al., 2002). The pERK expression can be used as a measure of the early event which occurred in dorsal horn neurons after noxious peripheral stimulation.

3.1. *Changes in digastric and masseteric muscle activities*

The digastric and masseteric muscles are activated by noxious stimulation of the tooth pulp (Park et al., 2001; Sunakawa et al., 1999). The EMG activity recorded from these muscles is a good indicator of noxious responses in the trigeminal system. We observed a significant increase in EMG activity of these muscles following capsaicin injection into the molar tooth pulp, but not following vehicle injection (Fig. 1). The increase in EMG activity lasted for about 3–5 min, although a significant difference was only detected within 1 min. The time-course change in EMG activity was similar to that of pERK expression following capsaicin treatment of the tooth pulp. These data strongly suggest that the increase in EMG activity and pERK expression after the capsaicin application to the tooth pulp should be a result of the activation of intra-pulpal high threshold afferents including C-fibers and an acute tooth pulp inflammation.

3.2. *pERK-LI cells in the Vi/Vc zone and Pa5*

It has been reported that glial cells in the spinal dorsal horn (DH) express pERK following peripheral inflammation (Zhuang et al., 2005). It may be possible that pERK is expressed in the glial cells of Vi/Vc and Vc/C2 zones after tooth pulp inflammation such as spinal DH. The expression of pERK in the glial cells is observed 1–2 weeks after inflammation, and those with pERK are distributed in the wide area of DH in both sides (Zhuang et al., 2005) The Vi/Vc and Vc/C2 neurons with pERK following capsaicin treatment of the tooth pulp were localized in the superficial laminae and were also ipsilateral dominant. These data strongly suggest that pERK-LI cells we observed after capsaicin tooth pulp treatment are expressed in the Vi/Vc and Vc/C2 neurons but not in glial cells. We observed a large number of pERK-LI cells in the dorsal portion of the Vi/Vc zone and Pa5 bilaterally following capsaicin injection into the upper or lower molar tooth pulp. Previous HRP tracing studies have reported that tooth pulp afferents were somatotopically arranged in the cat trigeminal nuclei (Sp5) (Shigenaga et al., 1986, 1989). Upper tooth pulp afferents project to the ventral portion of the Vc, whereas lower tooth pulp afferents were distributed in the dorsal portion of Vc. The distribution areas of pERK-LI cells within Vc and Pa5 following capsaicin injection into the tooth pulp were similar in the upper and lower molar tooth as illustrated in Fig. 3. The pERK-LI cells were not observed in the ventral portion of the Vi/Vc transition zone where Fos protein-LI cells were expressed following capsaicin injection into the upper molar tooth pulp (Fig. 7). The distribution area of pERK-LI cells in Vi/Vc zone and Pa5 was different from the results of Fos study where Fos protein-LI cells were bilaterally represented in the ventral Vi/Vc zone and Pa5. These results indicate that the Vi/Vc zone and Pa5 regions lack somatotopic organization for trigeminal nociception. It has been reported that Fos protein-LI cells are expressed in spinal DH 0.5–1.0 h following noxious stimulation of the skin, whereas pERK-LI cells are expressed within 10 min (Ji et al., 2002; Tokunaga et al., 1995). The time-course difference in expression between pERK and Fos protein may be reflected in the distribution differences of positive neurons in the Vi/Vc zone. It is probable that pERK activation is an earlier event in tooth pulp nociception in the region as compared with that of Fos.

It has been known that the topographical organization of nociceptive neurons in the Vc is an important factor in the discrimination of tooth pulp pain (Dubner et al., 1989; Price and Dubner, 1977). On the other hand, the capsaicin treatment of the whisker pad produces a large number of pERK-LI cells in the restricted area of the ipsilateral Vc. This region corresponds to the whisker pad primary afferent projection area in Vc (Takemura et al., 1991). These suggest that pERK-LI cells expressed in the Vi/Vc zone and Pa5 following tooth pulp stimulation would not be involved in the sensory discriminative aspect of tooth pulp pain, whereas those expressed after whisker pad stimulation may have a function to discriminate nociception of the facial skin. Some previous studies reported that Fos expression in Vi/Vc and Pa5 following temporomandibular inflammation was strongly affected by vagal nerve transection (Bereiter et al., 2002). These data and the present findings suggest that the Vi/Vc and Pa5 neurons are involved in autonomic regulation as well as trigeminal nociception.

3.3. *pERK expression in the Vc/C2 zone*

We observed a significant increase in pERK expression in the Vc/C2 ipsilaterally, whereas a few pERK-LI cells were observed in the contralateral Vc/C2 zone following capsaicin injection into the molar tooth pulp. We also observed many Fos protein-LI cells in this region 1 h after capsaicin injection into the upper molar tooth pulp. It has been reported that Fos protein-LI cells are strongly expressed in the ipsilateral Vc/C2 zone following TMJ inflammation, parotid gland inflammation or tooth pulp stimulation (Hathaway et al., 1995; Nomura et al., 2002; Ogawa et al., 2003; Zhou et al., 1999). Nociceptive neurons in the Vc/C2 zone may receive direct inputs from the TMJ, parotid gland or tooth pulp and exhibit increased neuronal activity following TMJ, parotid gland or tooth pulp inflammation. It is well known that peripheral inflammation produces an extensive increase in the excitability of small diameter primary afferent nerve fibers, resulting in hyperexcitability of the second order neurons (Chiang et al., 1998; Hylden et al., 1989; Zhou et al., 1999). We observed that the pERK-LI cells were differentially arranged in the Vc/C2 zone following upper or lower molar tooth pulp stimulation. Capsaicin injection into the upper tooth pulp induced a large number of pERK-LI cells in the lateral portion of the Vc/C2 zone, whereas capsaicin injection into the lower tooth pulp resulted in pERK-LI cells in the medial portion of Vc/C2 zone. A small number of pERK-LI cells were expressed after capsaicin injection into the whisker pad. The difference in the topographical arrangement of pERK-LI cells in Vc/C2 zone following different tooth pulp stimulation was consistent with topography of trigeminal afferents and a role for tooth pulp nociceptive neurons to discriminate tooth pulp pain.

It has been reported that the tooth-pulp-driven neurons are also recorded from the spinal trigeminal subnucleus oralis (Vo) (Park et al., 2001). Previous anatomical tracing studies have shown that there are direct projection fibers from the tooth pulp to the Vo as well as Vc in cats (Shigenaga et al., 1989). There may be two possible mechanisms to activate Vo neurons by tooth pulp stimulation as follows: the Vo neurons are directly activated by tooth pulp primary afferents or are activated by the afferent inputs through Vc neurons. We could not observe any pERK-LI cells in Vo following capsaicin stimulation of the tooth pulp. It is likely that Vc neurons are directly activated by capsaicin injection into the tooth pulp at the early time period following tooth pulp stimulation and Vo neurons receive high threshold tooth pulp inputs originated from the pulpal C- and Aδ-fiber afferents through Vi/Vc and/or Vc/C2 neurons.

We also observed a large number of pERK-LI cells in the Vi/Vc zone, Pa5 and Vc/C2 zone following vehicle injection into the tooth pulp. The dental paper points were used for application of vehicle into the tooth pulp. The pERK expression following vehicle injection into the pulp may be originated from the direct mechanical stimulation of the tooth pulp.

3.4. *Functional significance of pERK in tooth pulp pain*

The ERK activation is known as an important step in the MAP kinase cascade involved in the intracellular signal transduction (Ji et al., 1999, 2002). ERK is phosphorylated as a result of the activation of neurotransmitter receptors in the excitable membrane. C-fiber stimulation in peripheral structures activates the ERK pathway in primary afferent and dorsal horn neurons (Ji et al., 1999, 2002; Liu et al., 2004). The pERK expression was increased following an increase in the noxious stimulus intensity in these neurons (Dai et al., 2002; Ji et al., 1999). The present study shows that the capsaicin stimulation of the tooth pulp induced phosphorylation of ERK in the Vi/Vc zone, Pa5 and Vc/C2 zone neurons. The phosphorylation of ERK was observed immediately after the tooth pulp stimulation (within 1 min). It is known that the capsaicin application dominantly activates the C-fibers in peripheral structures (Guan et al., 2004; Lin et al., 2000). This indicates that the pERK expression in medulla observed in the present study is the result of the activation of the intra-pulpal C-fiber afferents. It is clear that the capsaicin stimulation activates primary afferent neurons, resulting in the activation of tooth-pulp-driven neurons in Vi/Vc zone, Pa5 and Vc/C2. Thus, an activation of intra-pulpal C-fiber afferents leads to intracellular signal transduction in tooth-pulp-driven neurons in the Vi/Vc zone and Pa5 and Vc/C2 zone via the intracellular ERK signal transduction pathway, resulting in the inflammation-induced tooth pulp pain.

4. Experimental procedures

This study was approved by the Animal Experimentation Committee at Nihon University School of Dentistry, and animal treatments were performed according to the guidelines of the International Association for the Study of Pain (Zimmerman, 1983). Sprague–Dawley male rats weighing between 250 and 350 g were used.

We divided the experimental rats in 7 groups depending on the treatment as follows: rats with capsaicin or vehicle-injected into the first upper molar, rats with capsaicin or vehicle-injected into the lower molar, rats with capsaicin or vehicle subcutaneously injected into the whisker pad and naive rats without any treatments.

4.1. *Electromyographic recording and capsaicin application*

The capsaicin or vehicle-treated rats (n = 5 in each group) were introduced for EMG recording experiments. All procedures were performed under sodium pentobarbital anesthesia (50 mg/kg, i.p.). Capsaicin (Wako Co. LTD) was dissolved in 100% ethanol and 7% Tween 80 in saline (10 mM) and injected into the upper right first molar pulp with the tip of paper points. The same amount of solvent (100% ethanol and 7% Tween 80 in saline (10 mM)) was used as a vehicle.

Anesthesia was initially induced by inhalation of 3.0% halothane mixed with oxygen, and a tracheal cannula was inserted. Animals were placed on a heating pad in the dorsal recumbent position. To allow for the application of capsaicin in the maxillary first molar, the rats' mouth was gently opened and the dental pulp was exposed by means of low-speed dental drill with a round tungsten carbide bur (No. 1–4) under water cooling. The pulp surface was covered with a small piece of cotton soaked with physiological saline until capsaicin was applied. After surgery, the halothane concentration was reduced (0.6–0.8%) until noxious pressure applied to the hind-paw could induce a weak flexion reflex of the hind limb to ensure that an adequate level of anesthesia was maintained during the experiment. The heart rate, percent of expired CO_2 concentration and body core temperature were continuously monitored throughout the experiment and kept within the physiological range. A pair of bipolar EMG electrodes (enamel-coated stainless steel wire, inter-polar distance: 5 mm) was inserted into the digastric and masseter muscles on the side ipsilateral to the chemical application. A rest period of 1–2 h was allowed after the surgery in order to obtain a stable baseline level of EMG activity. EMG activity in two jaw muscles was continuously monitored before, during and after the application of capsaicin into the molar tooth pulp. Capsaicin was applied to the tooth pulp by a small piece of dental paper point (diameter, 0.15 mm; length, 1.5 mm; PIERCE ABSORBENT POINTS, ISO size #15); the cavity was then quickly sealed with a small piece of cotton to prevent any possible leakage of capsaicin to the surrounding tissues. Before the application of capsaicin, the baseline EMG activity was monitored for 20 min, and, after the application of the chemical, the EMG activity was continuously monitored for an additional 20 min. The EMG activity from each muscle was amplified and rectified and integrated by the Spike 2 software (CED, Cambridge). The mean baseline level was determined by calculating the mean EMG area over the first 20 min prior to the injection of capsaicin into the tooth pulp. The area of the integrated EMG activity was measured for every 1 min, and mean EMG activity was calculated.

4.2. *pERK and Fos immunohistochemistries*

The procedure for capsaicin or vehicle treatment of the tooth pulp was same as EMG recording experiment. Fifty microliters of capsaicin or vehicle was injected into the whisker pad subcutaneously. After appropriate survival times (the survival time after capsaicin stimulation of the maxillary first molar: 2, 5, 10, 30, 120 min, n = 5 each group; 5 min after vehicle injection into the first upper or lower molar tooth pulp or subcutaneous injection into the whisker pad, n = 5 each group), rats were perfused through the aorta with 500 ml 0.9% saline followed by

500 ml 4% paraformaldehyde in 0.1 M phosphate buffer (PB, pH 7.4). The naive rats were anesthetized without any surgical treatment and perfused with the same procedure as tooth-pulp-treated rats. The whole brain including medulla and upper cervical cord was removed and post-fixed in the same fixative for 3 days at 4 °C. The tissues were then transferred to 20% sucrose (w/v) in phosphate-buffered saline (PBS) for several days for cryoprotection. Thirty-micron-thick sections were cut with a freezing microtome, and every fourth section was collected in PBS. Free-floating tissue sections were rinsed in PBS, 10% normal goat serum in PBS for 1 h, and then incubated in rabbit anti-phospho-p44/42 MAP Kinase Antibody (1:1000, Cell Signaling Technology) for 72 h at 4 °C. Next, the sections were incubated in biotinylated goat anti-rabbit IgG (1:600; Vector Labs, Burlingame, CA, USA) for 2 h at room temperature. After washing, the sections were incubated in peroxidase-conjugated avidin–biotin complex (1:100; ABC, Vector Labs) for 2 h at room temperature. After washing in 0.05 M Tris Buffer (TB), the sections were incubated in 0.035% 3,3′-diaminobenzidine-tetra HCl (DAB, Sigma), 0.2% nickel ammonium sulfate and 0.05% peroxide in 0.05 M TB (pH 7.4). The sections were washed in PBS, serially mounted on gelatin-coated slides, dehydrated in alcohols and cover slipped. For Fos immunohistochemistry, rats were perfused with same fixative used for pERK immunohistochemistry 60 min after capsaicin ($n = 5$) or vehicle ($n = 5$) injection into the upper molar tooth pulp. The medulla and the upper spinal cord were cut, and sections were rinsed in PBS, 3% normal goat serum (NGS) in PBS for 1 h, then incubated for 72 h with rabbit anti-c-fos (1:20,000: c-fos ab-5, Oncogene, MA, USA) in 3% NGS at 4 °C. The following immunohistochemical procedures were similar to those of pERK immunohistochemistry.

The pERK- or Fos protein-LI cells were drawn under the light microscope using camera-lucida drawing tube. The number of pERK- or Fos protein-LI cells was counted from every 8th section. The total number of pERK- or Fos protein-LI cells from three of every 8th section was calculated, and the mean number of pERK-LI cells (three sections/rat) was obtained from each animal in order to avoid the variability of the number of immunoreactive neurons in each section.

4.3. *Western blot*

Six rats with capsaicin or vehicle injection into the upper first molar tooth pulp (3 rats in each group) were used for Western blot analysis. Rats were anesthetized with sodium pentobarbital (50 mg/kg, i.p.), and upper molar tooth pulps were treated with capsaicin. Five minutes after capsaicin injection, rats were perfused with 500 ml of 0.1 M PB containing phosphatase inhibitor (40 mM NaF, 10 mM Na_3Vo_4 and 100 mM NaCl), and brainstem and upper cervical cord were removed. The upper half of the medulla and cervical cord were cut. Sections 1 mm rostral to 2 mm caudal from the obex (Vi/Vc zone and Pa5) and 4 to 8 mm caudal from the obex (Vc/C2 zone) were cut from the brainstem and upper cervical cord. Then, the lateral half of each section (ipsilateral and contralateral sides to capsaicin treatment) was taken for Western blot. The samples were immersed in 200 μl of homogenization buffer (50 mM Tris–HCl, pH 7.5/5 mM EGTA/1.4 μM β-mercaptoethanol/2 mM phenylmethylsulfonyl fluoride/0.2 mg/ml trypsin inhibitor) and homogenized by Dounce's homogenizer for 25 strokes. The homogenates were centrifuged at 14,000×*g* for 5 min, and the supernatants were transferred to fresh tubes. Ten micrograms of samples was loaded for 10% sodium dodecyl sulfate polyacrylamide gel electrophoresis (SDS-PAGE) and transferred to Immobilon-P transfer membrane (Millipore, Bedford, MA). The membranes were incubated in 1% (w/v) bovine serum albumin (BSA) in PBS/0.1% Tween 20 (BSA-PBST) for 1 h at room temperature to block the background reaction and then incubated with polyclonal rabbit anti-rat phospho-ERK, rabbit anti-rat nonphospho-ERK antibodies for 16 h at 4 °C. After washing in PBS containing 0.1% Tween 20 (PBST), the membranes were incubated with horseradish-peroxidase (HRP)-conjugated goat anti-rabbit IgG (H+L) (Jackson Immuno Research Laboratories, West Grove, PA) (1:10,000 dilution in BSA-PBST). The membranes were washed with PBST for three times and then incubated with ECL reagents (Amersham, Piscataway, NJ) for 1 min. The membranes were exposed to X-ray film (Kodak) for 2–5 min and developed. Autoradiograms were analyzed, and the intensity of immunoreactive bands of interest was quantified by densitometric analysis using NIH Image 1.60.

4.4. *Statistical analysis*

Statistical analysis was performed using analysis of variance (ANOVA) followed by Fisher's protected least-significant difference (LSD) test, Newmann–Keuls test, Dunnett's test or Scheffe tests. Student's *t* test or Welch's *t* test was also used as appropriate. Differences were considered significant at $p < 0.05$. Results are presented as means ± SD.

Acknowledgments

We thank Prof. R. Dubner for invaluable comments and Dr. D. A. Thomas for correcting English usage on the manuscript. This study was supported in part by Research grants from Sato and Uemura Funds from Nihon University School of Dentistry and Grant from Dental Research Center, Nihon University School of Dentistry; Nihon University multidisciplinary research grant and Individual Research Grant; a Grant from the Ministry of Education, Culture, Sports, Science and Technology to promote multidisciplinary research projects; a grant from the Ministry of Education, Culture, Sports, Science, and Technology to promote multidisciplinary research projects "Brain Mechanisms for Cognition, Memory and Behavior" at Nihon University. K.R. is supported by the NIH grant DE11964.

REFERENCES

Addy, M., Pearce, N., 1994. Aetiological, predisposing and environmental factors in dentine hypersensitivity. Arch. Oral Biol. 39, 33–38.

Bereiter, D.A., Bereiter, D.F., Ramos, M., 2002. Vagotomy prevents morphine-induced reduction in Fos-like immunoreactivity in trigeminal spinal nucleus produced after TMJ injury in a sex-dependent manner. Pain 96, 205–213.

Byers, M.R., 1984. Dental sensory receptors. Int. Rev. Neurobiol. 25, 39–94.

Byers, M.R., Narhi, M.V., 1999. Dental injury models: experimental tools for understanding neuroinflammatory interactions and polymodal nociceptor functions. Crit. Rev. Oral Biol. Med. 10, 4–39.

Caterina, M.J., Schumacher, M.A., Tominaga, M., Rosen, T.A., Levine, J.D., Julius, D., 1997. The capsaicin receptor: a heat-activated ion channel in the pain pathway. Nature 389, 816–824.

Chattipakorn, S.C., Light, A.R., Narhi, M., Maixner, W., 2001. The effects of noxious dental heating on the jaw-opening reflex and trigeminal Fos expression in the ferret. J. Pain 2, 345–353.

Chattipakorn, S.C., Sigurdsson, A., Light, A.R., Narhi, M., Maixner,

W., 2002. Trigeminal c-Fos expression and behavioral responses to pulpal inflammation in ferrets. Pain 99, 61–69.
Chiang, C.Y., Park, S.J., Kwan, C.L., Hu, J.W., Sessle, B.J., 1998. NMDA receptor mechanisms contribute to neuroplasticity induced in caudalis nociceptive neurons by tooth pulp stimulation. J. Neurophysiol. 80, 2621–2631.
Dai, Y., Iwata, K., Fukuoka, T., Kondo, E., Tokunaga, A., Yamanaka, H., Tachibana, T., Liu, Y., Noguchi, K., 2002. Phosphorylation of extracellular signal-regulated kinase in primary afferent neurons by noxious stimuli and its involvement in peripheral sensitization. J. Neurosci. 22, 7737–7745.
Dubner, R., Kenshalo Jr., D.R., Maixner, W., Bushnell, M.C., Oliveras, J.L., 1989. The correlation of monkey medullary dorsal horn neuronal activity and the perceived intensity of noxious heat stimuli. J. Neurophysiol. 62, 450–457.
Guan, Y., Guo, W., Robbins, M.T., Dubner, R., Ren, K., 2004. Changes in AMPA receptor phosphorylation in the rostral ventromedial medulla after inflammatory hyperalgesia in rats. Neurosci. Lett. 366, 201–205.
Hathaway, C.B., Hu, J.B., Bereiter, D.A., 1995. Distribution of Fos-like immunoreactivity in the caudal brainstem of the rat following noxious chemical stimulation of the temporomandibular joint. J. Comp. Neurol. 356, 444–456.
Hu, J.W., Sessle, B.J., 1984. Comparison of responses of cutaneous nociceptive and nonnociceptive brain stem neurons in trigeminal subnucleus caudalis (medullary dorsal horn) and subnucleus oralis to natural and electrical stimulation of tooth pulp. J. Neurophysiol. 52, 39–53.
Hu, J.W., Dostrovsky, J.O., Sessle, B.J., 1981. Functional properties of neurons in cat trigeminal subnucleus caudalis (medullary dorsal horn). I. Responses to oral–facial noxious and nonnoxious stimuli and projections to thalamus and subnucleus oralis. J. Neurophysiol. 45, 173–192.
Hylden, J.L., Nahin, R.L., Traub, R.J., Dubner, R., 1989. Expansion of receptive fields of spinal lamina I projection neurons in rats with unilateral adjuvant-induced inflammation: the contribution of dorsal horn mechanisms. Pain 37, 229–243.
Iwata, K., Takahashi, O., Tsuboi, Y., Ochiai, H., Hibiya, J., Sakaki, T., Yamaguchi, Y., Sumino, R., 1998. Fos protein induction in the medullary dorsal horn and first segment of the spinal cord by tooth-pulp stimulation in cats. Pain 75, 27–36.
Iwata, K., Tsuboi, Y., Shima, A., Harada, T., Ren, K., Kanda, K., Kitagawa, J., 2004. Central neuronal changes after nerve injury: neuroplastic influences of injury and aging. J. Orofac. Pain 18, 293–298.
Ji, R.R., Baba, H., Brenner, G.J., Woolf, C.J., 1999. Nociceptive-specific activation of ERK in spinal neurons contributes to pain hypersensitivity. Nat. Neurosci. 2, 1114–1119.
Ji, R.R., Befort, K., Brenner, G.J., Woolf, C.J., 2002. ERK MAP kinase activation in superficial spinal cord neurons induces prodynorphin and NK-1 upregulation and contributes to persistent inflammatory pain hypersensitivity. J. Neurosci. 22, 478–485.
Jyvasjarvi, E., Kniffki, K.D., 1992. Studies on the presence and functional properties of afferent C-fibers in the cat's dental pulp. Proc. Finn. Dent. Soc. 88, 533–542.
Kawasaki, Y., Kohno, T., Zhuang, Z.Y., Brenner, G.J., Wang, H., Van Der Meer, C., Befort, K., Woolf, C.J., Ji, R.R., 2004. Ionotropic and metabotropic receptors, protein kinase A, protein kinase C, and Src contribute to C-fiber-induced ERK activation and cAMP response element-binding protein phosphorylation in dorsal horn neurons, leading to central sensitization. J. Neurosci. 24, 8310–8321.
Lin, Q., Zou, X., Willis, W.D., 2000. Adelta and C primary afferents convey dorsal root reflexes after intradermal injection of capsaicin in rats. J. Neurophysiol. 84, 2695–2698.
Liu, Y., Obata, K., Yamanaka, H., Dai, Y., Fukuoka, T., Tokunaga, A., Noguchi, K., 2004. Activation of extracellular signal-regulated protein kinase in dorsal horn neurons in the rat neuropathic intermittent claudication model. Pain 109, 64–72.
Narhi, M., Jyvasjarvi, E., Virtanen, A., Huopaniemi, T., Ngassapa, D., Hirvonen, T., 1992. Role of intradental A- and C-type nerve fibres in dental pain mechanisms. Proc. Finn. Dent. Soc. 88, 507–516.
Narhi, M.V., Yamamoto, H., Ngassapa, D., Hirvonen, T., 1994. The neurophysiological basis and the role of inflammatory reactions in dentine hypersensitivity. Arch. Oral Biol. 39, 23–30.
Nomura, H., Ogawa, A., Tashiro, A., Morimoto, T., Hu, J.W., Iwata, K., 2002. Induction of Fos protein-like immunoreactivity in the trigeminal spinal nucleus caudalis and upper cervical cord following noxious and non-noxious mechanical stimulation of the whisker pad of the rat with an inferior alveolar nerve transection. Pain 95, 225–238.
Oakden, E.L., Boissonade, F.M., 1998. Fos expression in the ferret trigeminal nuclear complex following tooth pulp stimulation. Neuroscience 84, 197–208.
Obata, K., Yamanaka, H., Dai, Y., Mizushima, T., Fukuoka, T., Tokunaga, A., Noguchi, K., 2004a. Differential activation of MAPK in injured and uninjured DRG neurons following chronic constriction injury of the sciatic nerve in rats. Eur. J. Neurosci. 20, 2881–2895.
Obata, K., Yamanaka, H., Kobayashi, K., Dai, Y., Mizushima, T., Katsura, H., Fukuoka, T., Tokunaga, A., Noguchi, K., 2004b. Role of mitogen-activated protein kinase activation in injured and intact primary afferent neurons for mechanical and heat hypersensitivity after spinal nerve ligation. J. Neurosci. 24, 10211–10222.
Ogawa, A., Ren, K., Tsuboi, Y., Morimoto, T., Sato, T., Iwata, K., 2003. A new model of experimental parotitis in rats and its implication for trigeminal nociception. Exp. Brain Res. 152, 307–316.
Park, S.J., Chiang, C.Y., Hu, J.W., Sessle, B.J., 2001. Neuroplasticity induced by tooth pulp stimulation in trigeminal subnucleus oralis involves NMDA receptor mechanisms. J. Neurophysiol. 85, 1836–1846.
Pertovaara, A., Huopaniemi, T., Aukee, K., Carlson, S., 1987. Tooth pulp-evoked activity in the spinal trigeminal nucleus caudalis of cat: comparison to primary afferent fiber, reflex, and sensory responses. Exp. Neurol. 95, 155–166.
Price, D.D., Dubner, R., 1977. Neurons that subserve the sensory-discriminative aspects of pain. Pain 3, 307–338.
Sessle, B.J., 1987. The neurobiology facial and dental pain: present knowledge, future directions. J. Dent. Res. 66, 962–981.
Sessle, B.J., Greenwood, L.F., 1976. Inputs to trigeminal brain stem neurons from facial, oral, tooth and pharyngolaryngeal tissues: I. Responses to innocuous and noxious stimuli. Brain Res. 117, 211–226.
Sessle, B.J., Hu, J.W., Amano, N., Zhong, G., 1986. Convergence of cutaneous, tooth pulp, visceral, neck and muscle afferents onto nociceptive and non-nociceptive neurons in trigeminal subnucleus caudalis (medullary dorsal horn) and its implications for referred pain. Pain 27, 219–235.
Shigenaga, Y., Suemune, S., Nishimura, M., Nishimori, T., Sato, H., Ishidori, H., Yoshida, A., Tsuru, K., Tsuiki, Y., Dateoka, Y., 1986. Topographic representation of lower and upper teeth within the trigeminal sensory nuclei of adult cat as demonstrated by the transganglionic transport of horseradish peroxidase. J. Comp. Neurol. 251, 299–316.
Shigenaga, Y., Nishimura, M., Suemune, S., Nishimori, T., Doe, K., Tsuru, H., 1989. Somatotopic organization of tooth pulp primary afferent neurons in the cat. Brain Res. 477, 66–89.
Sugimoto, T., He, Y.F., Funahashi, M., Ichikawa, H., 1998. Induction of immediate-early genes c-fos and zif268 in the subnucleus oralis by noxious tooth pulp stimulation. Brain Res. 794, 353–358.

Sunakawa, M., Chiang, C.Y., Sessle, B.J., Hu, J.W., 1999. Jaw electromyographic activity induced by the application of algesic chemicals to the rat tooth pulp. Pain 80, 493–501.

Takemura, M., Sugimoto, T., Shigenaga, Y., 1991. Difference in central projection of primary afferents innervating facial and intraoral structures in the rat. Exp. Neurol. 111, 324–331.

Tokunaga, A., Doi, M., Senba, E., 1995. Effects of local anaesthesia on formalin-induced Fos expression in the rat dorsal horn. NeuroReport 6, 2301–2304.

Wang, H., Dai, Y., Fukuoka, T., Yamanaka, H., Obata, K., Tokunaga, A., Noguchi, K., 2004. Enhancement of stimulation-induced ERK activation in the spinal dorsal horn and gracile nucleus neurons in rats with peripheral nerve injury. Eur. J. Neurosci. 19, 884–890.

Zhou, Q., Imbe, H., Dubner, R., Ren, K., 1999. Persistent Fos protein expression after orofacial deep or cutaneous tissue inflammation in rats: implications for persistent orofacial pain. J. Comp. Neurol. 412, 276–291.

Zhuang, Z.Y., Gerner, P., Woolf, C.J., Ji, R.R., 2005. ERK is sequentially activated in neurons, microglia, and astrocytes by spinal nerve ligation and contributes to mechanical allodynia in this neuropathic pain model. Pain 114, 149–159.

Zimmerman, M., 1983. Ethical guidelines for investigation of experimental pain in conscious animals. Pain 16, 109–110.